https://doi.org/10.5194/egusphere-2026-3739
Preprint. Discussion started: 2 July 2026

Spatial and temporal patterns of fracture in confined landfast sea ice

Ada Loewen[1], Derek Mueller[1], Gregory Crocker[1], Katherine Wilson[2], Adrianne Mike-Qaunaq[2], and Andrew R. Mahoney[3]

[1]Department of Geography and Environmental Studies, Carleton University, Ottawa, ON, Canada
[2]SmartICE Monitoring and Information Inc., St. John's, NL, Canada
[3]Geophysical Institute, University of Alaska Fairbanks, Fairbanks, AK, USA

Correspondence: Ada Loewen (adaloewen@cmail.carleton.ca)

Abstract.

Fractures in sea ice form when internal ice stresses exceed ice strength. The locations of recurring fractures in landfast sea ice are well known to Arctic Indigenous communities, but recent observations suggest changes in their timing and frequency driven by changes in the Arctic climate. Fractures affect sea ice stability, travel safety, and ocean-atmosphere exchanges, so understanding why, when, and where they occur is increasingly important with climate change. To improve predictions of fracturing and support safe travel, we analyze fracture patterns in Admiralty Inlet, Nunavut, Canada, a semi-enclosed waterway. Using satellite imagery from 2018 to 2023 and guided by Inuit Knowledge of recurring fracture zones, we examine how geographic, atmospheric, and oceanographic factors shape fracture behaviour. This study provides the first assessment of fracturing in a semi-enclosed landfast ice environment in the Canadian Arctic Archipelago, extending previous work focused on open-coast environments. We find that seasonal changes in ice properties such as ice thickness, temperature, and porosity largely control fracture timing. Our results further indicate that episodic high-stress events such as wind storms are not primary drivers; instead, stable geographic features such as points of land concentrate stress and govern fracture locations. These findings highlight the need for in-situ measurements of ice strength, under-ice currents, and sea surface height, as well as higher temporal resolution fracture monitoring. By integrating remote sensing, environmental datasets, and Inuit knowledge, this work advances understanding of landfast ice stability and improves predictive capabilities relevant to both community travel safety and Arctic climate modelling.

1 Introduction

Sea ice is a dynamic material that deforms and fractures when external or internal stresses exceed its capacity to accommodate strain (Weiss et al., 2007). Although sea ice strongly reduces the exchange of heat, moisture, and momentum between the atmosphere and ocean, fractures create openings where these interactions can occur, influencing local ice melt, ocean mixing, and atmospheric conditions (Marcq and Weiss, 2012). Once formed, fractures may remain open and lengthen or widen over time, refreeze in place, or close due to convergent motion and form pressure ridges (Petrich et al., 2007; Laidler et al., 2008; Laidler and Ikummaq, 2008). The characteristics of fractures and the processes that lead to their formation depend on the physical properties of the ice (e.g., thin vs. thick, warm vs. cold) and the geographical setting (e.g., pack ice vs. confined

https://doi.org/10.5194/egusphere-2026-3739
Preprint. Discussion started: 2 July 2026

coastal regions). In addition, a range of environmental factors drive the formation and evolution of fractures, including wind, ocean currents, tides, bathymetry, and waves (Willmes et al., 2023; Kovalev et al., 2020; Hui et al., 2016; Reiser et al., 2019). Pan-Arctic temporal trends in fracture coverage are unclear due to methodological challenges with identifying fractures in thermal imagery (Hoffman et al., 2022; Willmes and Heinemann, 2016). However, regional fracture inventories have indicated increasing trends of fracture coverage in certain regions in the Arctic due to warming air temperatures and changes in synoptic weather patterns (Qu et al., 2021).

Fractures can be classified based on their width, length, location relative to geographical features, or processes that led to their formation. To standardize the terminology used to describe fractures and other sea ice features, the World Meteorological Organization (WMO) has developed an internationally recognized sea ice nomenclature (WMO, 2014). This classification system supports forecasting, shipping, ice charting, and scientific research, with a focus on spatial scales relevant to maritime navigation. In contrast, Arctic Indigenous communities use detailed, locally developed terms for sea ice, including various types of fractures, that reflect spatial and temporal scales important for safe on-ice travel and subsistence activities (Wilson et al., 2021; Heyes, 2011; Laidler et al., 2009; Krupnik, 2011). While these unique vocabularies focus on different applications and temporal and spatial scales, bringing them together builds a more comprehensive understanding of fracture dynamics.

Despite long-standing observations by Inuit communities of recurring fracture locations and patterns (Laidler et al., 2010), the underlying causes and variability of these features remain poorly understood by both Inuit and academics. Scientific models fail to accurately represent fracture properties in pack ice such as angle and length, in part due to uncertainties in how sea ice behaves across different spatial and temporal scales (Hutter et al., 2022). For landfast ice in confined coastal settings, such as those found in the Canadian Arctic Archipelago, the influence of shorelines and pinning points such as islands and promontories (points of land) introduces additional complexity in understanding and modelling the physical processes that govern fracture formation and evolution (Lemieux et al., 2016; Liu et al., 2022). Currently, there is a lack of both *in-situ* and remote sensing observations of fractures in landfast ice, limiting our ability to characterize the unique patterns and drivers of fracture formation in these regions. This gap is particularly critical given the reliance on sea ice for travel and subsistence in coastal Arctic communities, and recent changes in the climate altering atmospheric and oceanographic patterns which lead to fracture formation (Ford et al., 2019).

Community members in Ikpiarjuk (Arctic Bay), Nunavut are increasingly concerned about changes in sea ice characteristics in Admiralty Inlet, which have been affecting ice travel safety. In particular, travel to the floe edge, the edge of the landfast ice which initially forms at the mouth of Admiralty Inlet and gradually progresses south in the spring, is a major concern (Bell et al., 2019; Archer et al., 2017). The floe edge is a highly biologically productive area and an important narwhal hunting location for Ikpiarjukmiut (Inuit from Ikpiarjuk) and a tourism venue (Archer et al., 2017). Fractures create several types of hazards for sea ice travellers going to the floe edge. Travellers from Ikpiarjuk must cross several large fractures ($\sim$1-10 m wide) on their way to the floe edge in the spring. In addition, fractures influence where large pieces of ice can break off from the floe edge, potentially stranding travellers (Loewen et al., 2025). It has become more difficult for sea ice travellers to anticipate where fractures will form due to a combination of climate change, and disruptions in intergenerational knowledge transfer within Inuit communities (Archer et al., 2017; Wilson et al., 2021).

https://doi.org/10.5194/egusphere-2026-3739
Preprint. Discussion started: 2 July 2026

To address these challenges, we have worked collaboratively with Tuvaliriji, the SmartICE community management committee in Ikpiarjuk. SmartICE is a social enterprise that partners with northern Indigenous communities to augment Indigenous and local knowledge of ice with environmental monitoring technology and satellite imagery (see www.smartice.org). Tuvaliriji consists of members from the local Hunters and Trappers Organization, Hamlet council, Search and Rescue Committee, youth, Elders, and the local outfitter, Arctic Bay Adventures. Tuvaliriji contributed key knowledge that guided the identification of research questions, shaped data collection strategies, and informed the interpretation of fracturing processes alongside scientific analyses. In the first phase of this research, we developed a method for interpreting interferometric synthetic aperture radar (InSAR) and true-colour satellite imagery using both Inuit Knowledge and knowledge of sea ice remote sensing properties (Loewen et al., 2026).

Here, we use the resulting fracture dataset from Loewen et al. (2026) to investigate the spatial and temporal patterns of fracture formation in confined landfast sea ice in Admiralty Inlet, Nunavut. We aim to synthesize and explain these patterns by integrating Inuit Knowledge with current academic understanding of sea ice fracture mechanics alongside ancillary geographical, meteorological, and oceanographic data. In doing so, we provide an overview of what is currently known about fracture formation at community-relevant scales, identify features that deviate from recurring patterns, and propose hypotheses about their potential drivers, including sensitivities to future climate-driven change. Our results offer an additional source of information that can be used operationally within Northern communities, not as a replacement for Inuit Knowledge, but as a complementary tool that individuals may draw upon alongside their own observations and experience when evaluating sea-ice conditions and making travel decisions (Beaulieu et al., 2023; Simonee et al., 2021).

The structure of this paper is as follows: in Section 2, we summarize the current academic scientific literature on sea ice fracture dynamics, and in Section 3, we present local Inuit science of sea ice fracture behaviour in Admiralty Inlet, Nunavut. Section 4 describes the datasets used in this study, followed by our analytical methods: identifying spatial and temporal fracture patterns (Sections 5.1 and 5.2) and linking those patterns to ice properties, environmental stresses, and geographic conditions (Section 5.3). In Section 6.1, we report our spatial and temporal fracture pattern results. Section 6.2 presents seasonal estimates of ice strength, thermal stresses, wind and current stress magnitudes, and quantifies relationships between fracture locations and promontory points, side-inlet mouths, and river mouths. Finally, in Section 7, we discuss potential driving forces of the observed spatial and temporal patterns and identify opportunities to address remaining knowledge and data gaps.

2 Fracture of landfast ice

We can get a basic understanding of the balance of forces acting in landfast ice and how they relate to fracture by examining the standard sea ice momentum equation which considers only in-plane stresses (compressive, tensile, and shear) and can be written as the balance between the internal stress tensor and external forcings:

$$\nabla \cdot \sigma = \tau_{\mathbf{a}} + \tau_{\mathbf{o}} - \rho_i h g \nabla H_d + \tau_{\mathbf{b}} + \tau_{\mathbf{l}} \quad (1)$$

https://doi.org/10.5194/egusphere-2026-3739
Preprint. Discussion started: 2 July 2026

where σ is the internal ice stress tensor, τ_a and τ_o, are atmospheric (wind) and oceanic (current) drag, ρ_i is the density of the ice, h the mean ice thickness, g is acceleration due to gravity, H_d the sea-surface dynamic height, and τ_b and τ_l are basal and lateral stress terms. This equation is simplified from the full sea ice momentum equation by assuming the ice velocity is approximately zero and landfast ice is in static equilibrium (Liu et al., 2022)

This equation shows that the stresses within the ice must balance the applied wind and current drag, basal and lateral resisting forces (e.g. anchor points or coastal geometry) and large-scale changes in sea surface height. These terms are affected by the characteristics of both the ice and the surrounding environment, which vary seasonally and can be highly localized in space and time. We summarize some of the spatial and temporal characteristics of each of the factors we introduce below in Figure 1.

For example, the applied wind and ocean drag terms (τ_k where k is a for wind stresses or o for current stresses) can be estimated by the following equation:

$$\tau_k = c_k \, \rho_k \, u_k^2 \tag{2}$$

where c_k is the drag coefficient for air/water, ρ_k is the density of air/water, and u_k is the wind or current speed. c_k depends on the roughness of upper and lower surfaces of the ice and the size of the ice floe (Lu et al., 2011; Petty et al., 2017). Wind speeds are affected by topography, synoptic weather systems, and atmospheric stability (Moore and Imrit, 2022). Ocean currents are affected by tides, bathymetry, density-driven (baroclinic) flows, and larger-scale circulation patterns (Timmermans and Marshall, 2020). In addition, the pressure gradient force is affected by large-scale changes in sea surface height due to factors such as storm surges, tides, and barotropic and baroclinic ocean pressure gradients (Lemieux et al., 2018).

Several physical mechanisms can lead to the formation and maintenance of landfast ice, which are represented in sea ice models through parametrizations such as basal and lateral stress terms and boundary conditions. Basal stresses occur in shallow water when ice keels or pressure ridges become grounded, as commonly observed along the Alaska North Slope and in the Laptev Sea (Mahoney et al., 2007; Lemieux et al., 2016). Lateral stresses and coastal boundary conditions represent the stabilizing effect of pinning points due to island chains and coastal geometry that prevent ice motion in both deep and shallow waters (Liu et al., 2022). Anchoring forces can change throughout the ice season, increasing as ridges form and grow (Mahoney et al., 2007), and decreasing as nearshore ice preferentially melts due to enhanced heat inputs from the land (Loewen et al., 2025). Any stresses that are not balanced by external and resisting forces are accommodated by mechanical stress and fracturing within the ice.

In addition to the mechanical forces described above, temperature changes within the ice can generate thermal stresses (Lewis et al., 1994). Assuming the ice is totally confined (i.e., all thermal strain is transformed to internal stress) and responds to thermal stresses completely elastically (i.e., ignoring thermal relaxation, creep, and anisotropic material properties), thermal stresses ($\sigma_{thermal}$) can be estimated by the following equation:

$$\sigma_{thermal} = -E \, \alpha \, \Delta T \tag{3}$$

https://doi.org/10.5194/egusphere-2026-3739
Preprint. Discussion started: 2 July 2026

where E is Young's modulus, α is the thermal expansion coefficient, and ΔT is the vertical temperature gradient within the ice (Hata and Tremblay, 2015). In general, cooling causes contraction, while warming causes expansion, but the magnitude and sign of the thermal expansion coefficient can change depending on the ice temperature (Kaidel et al., 2025). Thermal stresses can be significant in landfast ice in confined waterways which prevents the stress to be accommodated by strain, leading to the formation of thermal cracks (Teigen et al., 2005; Fedders et al., 2024). Thermal cracks most likely form during rapid air temperature changes (i.e., over several hours), such as during the passage of a frontal system (Evans and Untersteiner, 1971), while snow cover can attenuate the effects of upper surface heat fluxes (Bigdeli et al., 2020).

Bending stresses due to waves and tides are not captured in the sea ice momentum equation but can be modelled separately and play a role in ice fracture (Langhorne et al., 2001; Fox and Squire, 1994; Voermans et al., 2021). As waves travel through ice, they attenuate according to the wave period and ice characteristics. Wind waves (periods 1-10 s) attenuate within a few kilometres of the landfast ice edge, while longer period waves (e.g., >10 s) can propagate further from the ice edge (Mahoney et al., 2016; Voermans et al., 2021). Tides also produce bending forces in sea ice, but over longer time (several hours) and spatial (entire ice sheet) scales. Greater bending curvature and thus tidal flexure will occur closer to grounded points.

Ice stresses can result in deformation. For stresses below the failure criterion and no pre-existing failure, deformation occurs as continuous strain, but if the yield is exceeded, the ice will fracture and deformation will be discontinuous (Weiss, 2013). Once a fracture develops, stress is relieved along the fracture plane, but concentrates in the ice surrounding the end of the fracture (i.e., the crack tip) (Dempsey et al., 2018). This can cause the fracture to propagate horizontally across the ice or vertically through the ice thickness (Lewis, 1995). Fractures may extend partially through the thickness of the ice (dry crack) or through the full thickness of the ice (wet crack). These features may form instantaneously due to a high-stress event or fatigue failure under cyclic loading (Jewell et al., 2023; Langhorne et al., 2001). Although the general principles of fracture mechanics are well established, the application of these mechanisms to sea ice fracture initiation, propagation, widening, and healing and the spatial and temporal scales at which they operate remain poorly understood due to challenges in observing these processes at appropriate temporal and spatial scales.

In addition to the stresses imposed on the ice, the strength of sea ice controls its failure behaviour. Ice strength can be estimated from its temperature, porosity (brine volume fraction), and structural characteristics, and, at larger scales, thickness, which can vary spatially and temporally (Timco and Weeks, 2010; Johnston, 2006). Throughout the season, the ice grows, melts, and undergoes thermal changes, which can be estimated from empirical observations or from thermodynamic modelling. Spatial variations in mechanical properties may predispose certain regions of the ice cover to fracture more readily under external stresses by causing stress concentrations (Dempsey et al., 2018; Weiss and Dansereau, 2017). For first-year landfast ice in sheltered locations, ice growth is primarily thermodynamically-driven (Li et al., 2020), so spatial gradients in ocean currents and snow cover can affect the air-ice-ocean energy balance and thus cause spatial variations in ice properties. Mechanical processes such as ridging may also affect ice properties, but this process is not as important in confined ice regions like Admiralty Inlet.

Despite its importance, few measurements of ice strength (e.g., tensile, compressive, flexural) are available (Timco and Weeks, 2010). Laboratory measurements tend to overestimate ice strength relative to geophysical scale measurements, roughly

https://doi.org/10.5194/egusphere-2026-3739
Preprint. Discussion started: 2 July 2026

by an order of magnitude (hundreds vs tens of kPa) (Weiss and Dansereau, 2017). This is thought to be due to (1) the lack of pre-existing flaws and microcracks in laboratory-grown ice, and (2) smaller defects requiring higher stresses for activation, which is a length scale effect (Lewis et al., 1994; Schulson and Hibler, 1991; Weiss et al., 2007). Efforts to link scales in sea ice mechanics are ongoing (Weiss and Dansereau, 2017; Bouchat et al., 2022; Hunke et al., 2020).

Ice fracturing is also influenced by episodic atmospheric and oceanic processes. Episodic events that last several hours up to a couple of days can induce significant short-term stresses in the ice that can initiate failure. For example, the passage of frontal systems can cause rapid air temperature changes and increased thermal stress (Lewis et al., 1994); abrupt shifts in wind patterns can increase wind stress (Jewell et al., 2023); and short-term sea surface level changes can increase bending stress and/or decrease grounding forces (Jones et al., 2016).

We suggest that geographical factors can regularly concentrate stresses in certain locations throughout the year, leading to the formation of fractures in recurring locations (e.g. promontory points, bathymetry). Episodic events can cause variability in these general locations or the timing of fracture formation. Together, these physical mechanisms shape when and where fractures occur, yet they only partly explain the spatial regularity and evolution of fractures in landfast ice. Inuit Knowledge provides a parallel body of evidence that integrates observations of local geography, weather, tidal cycles, and ice characteristics accumulated over generations to understand fracture behaviour (Laidler, 2006). This knowledge helps interpret fracture patterns that may not be easily captured by physics-based models alone.

3 Inuit Knowledge of fractures and changes in fracture evolution

Navigating sea ice by dog sled or snowmobile requires intimate knowledge of ice features such as fractures and ridges. Inuit Qaujimajatuqangit, or Inuit knowledge and values, represents a complex and locally-grounded understanding of environmental processes, including hazardous ice conditions. Fractures in landfast ice form along sea ice trails used by coastal Arctic communities, sometimes widening to over 10 m and becoming difficult or dangerous to cross (Laidler, 2006; Qikiqtani Inuit Association, 2013). By observing sea ice *in-situ* and sharing accumulated knowledge over generations, a deep and rich understanding of local sea ice dynamics becomes embedded in Inuit Knowledge, culture, and language. This knowledge broadens scientific understandings of environmental processes, due to the long period of observations over a localized spatial scale (Laidler, 2006).

Here, we provide a brief summary of the seasonal cycle of ice fracturing in Admiralty Inlet known to Ikpiarjukmiut, which are corroborated by Inuit Knowledge from other communities in the Arctic (Laidler and Elee, 2008; Laidler and Ikummaq, 2008; Laidler et al., 2008; Wilson et al., 2021; Heyes, 2011; Segal et al., 2020). This knowledge was shared by Tuvaliriji over ten workshops held between 2019 and 2025 in Ikpiarjuk held by SmartICE partners and me, and is documented by Tuvaliriji Committee et al. (2025); Bell et al. (2019). Specific Inuktitut terminology, which can vary by community, has been developed to allow Inuit to concisely express complex relationships between elements within the sea ice environment and communicate hazards while travelling on the ice (Laidler et al., 2008). We include sea ice terminology used by Ikpiarjukmiut to describe key sea ice features common in Admiralty Inlet.

https://doi.org/10.5194/egusphere-2026-3739
Preprint. Discussion started: 2 July 2026

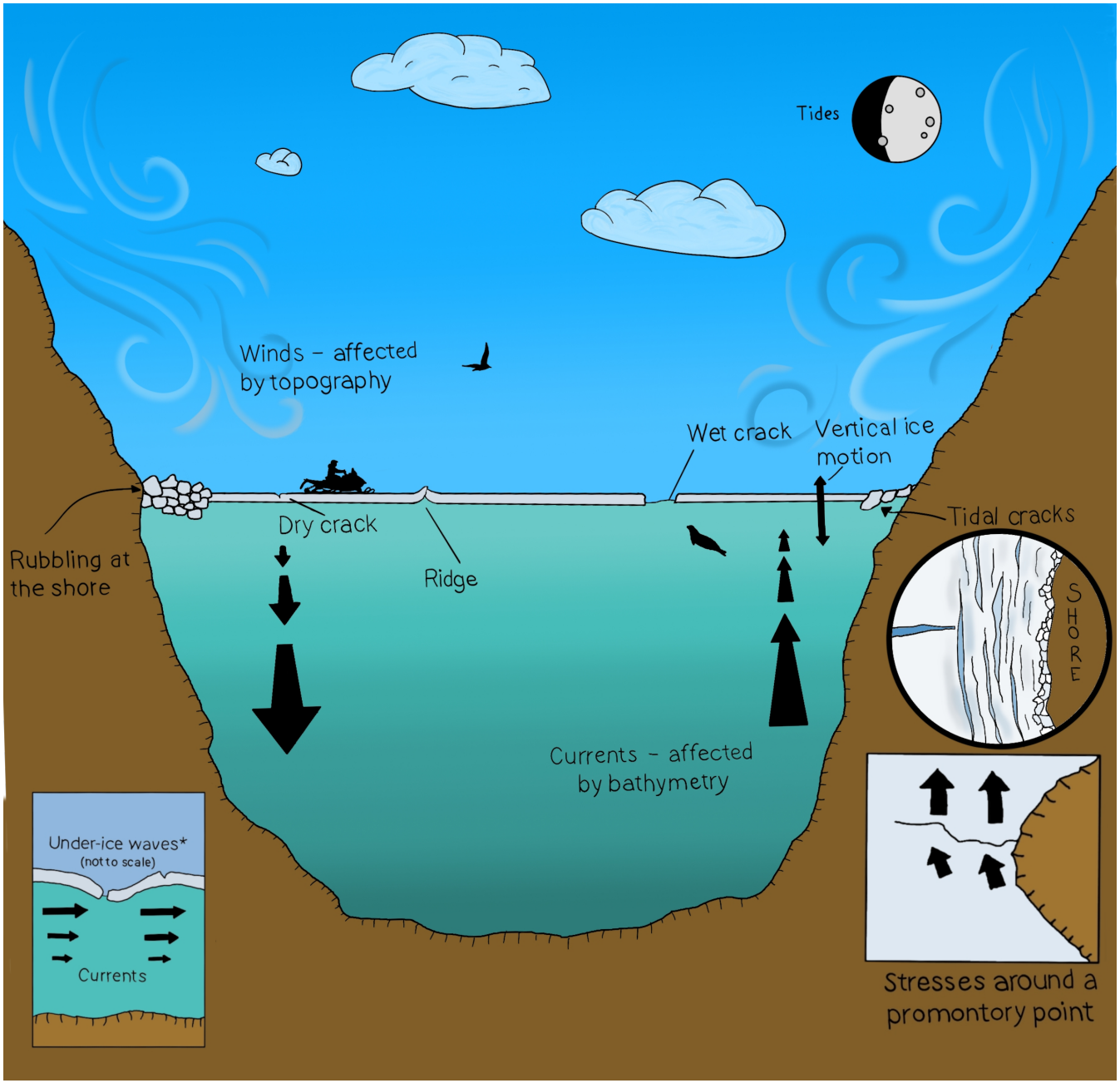

Figure 1. Conceptual diagram of processes that can lead to fracture formation in Admiralty Inlet. Illustration by Adrianne Mike-Qaunaq.

https://doi.org/10.5194/egusphere-2026-3739
Preprint. Discussion started: 2 July 2026

In the normal seasonal progression, sea ice undergoes multiple stages of thickening and consolidation into landfast ice. Sea ice typically begins to form in October to November, with interannual variability, and reaches a maximum thickness of approximately 2 m by May (Archer et al., 2017; Kowal et al., 2023; Environment and Climate Change Canada, 2026). Fractures form, freeze, and reopen throughout the ice season, and often occur near points of land, although this is not always the case. Two main types of fractures can form in the winter: *naggutiit* (singular: *nagguti*), which are considered 'wet cracks' because they extend through the full ice thickness, and *nuttaq*, which are 'dry cracks,' or surface fractures that do not go through the entire ice column. *Naggutiit* form throughout the winter due to significant temperature changes or tidal fluctuations in sea surface height and ocean currents, especially around full and new moon (i.e., during spring tide). *Naggutiit* may open and refreeze multiple times throughout the winter, or close and form ridges (*quglungniq*). *Agluit* (seal holes) are often created in *naggutiit* that have (re)opened, as seals use these locations repeatedly.

Later in the season, *aajurait* (singular: *aajuraaq*) form, which are fractures that open and remain open in spring. *Aajurait* may form at the same locations as *naggutiit* that formed in the winter, but they may also follow different paths. Both *naggutiit* and *aajurait* can be dangerous to cross when they are covered with snow (a feature called *anniruti*), which makes them difficult to see. In Ikpiarjuk, sea ice travellers look for *pilagiaqniq*, bridges of stable ice that form between the ends of *aajurait* and provide safe crossing points.

Several forms and stages of melt occur in spring (May and June). First, the snow melts, producing *puktailaq* (melt rivers and ponds) that reduce surface albedo, increase solar radiation absorption, and accelerate surface melting. Meltwater eventually drains through *aajurait* and *agluit*, and the ice becomes detached from the shore and free-floating (*tikpaqtuq*). We highlight that once the ice becomes *tikpaqtuq*, it does not necessarily drift away immediately. Rather, it becomes more susceptible to motion due to atmospheric and oceanic forcings. New fractures, *nuttaq* or *aajurait*, form at this time, indicating that the ice is increasingly unsafe to travel on and approaching break-up. A second stage of surface flooding from surface melting of the ice (*itisiuraq*) used to occur more frequently, but because the ice has thinned in recent years and break-up now happens earlier, this melt stage no longer typically develops.

In Admiralty Inlet, the floe edge is a key location for spring narwhal hunting, which provides a source of economic income for Ikpiarjukmiut (Archer et al., 2017). Ikpiarjukmiut have several concerns related to fractures. For one, travelling to the floe edge requires crossing several *aajurait*. To safely cross a wide *aajuraaq*, one must identify the feature, and stop before crossing to identify the ideal location to cross. Experienced travellers know where to anticipate fractures related to certain landmarks, but inexperienced travellers may not know to slow down where fractures are likely to occur. The locations of recurring fractures around several communities have been identified and documented to support safe travel (Laidler et al., 2008, 2009; Laidler and Elee, 2008; Wilson et al., 2021; Heyes, 2011). However, even experienced travellers need to be attentive for fractures, as the exact locations of fracture formation will change from year to year. In recent years, fractures have been forming in unanticipated locations around Admiralty Inlet. This is thought to be related to the thinning of sea ice in Admiralty Inlet, driven by a shortening ice season associated with climate change (Archer et al., 2017; Kowal et al., 2023). In addition, ice at the floe edge can become unstable, and if the environmental conditions allow, pieces of ice can detach and drift away which can be hazardous for hunters working at the floe edge. Usually these pieces of ice detach from the locations of pre-existing

https://doi.org/10.5194/egusphere-2026-3739
Preprint. Discussion started: 2 July 2026

aajurait (Loewen et al., 2025), so it is recommended for hunters to camp south of the northern-most *aajurait* if staying at the floe edge for an extended period of time.

Inuit Knowledge of sea ice has been built through generations of close observation of local environmental conditions and ice behaviour. This long-term, place-based expertise provides insights into recurring fracture patterns and environmental cues that are difficult to capture through short-term scientific observations alone. By collaborating with Inuit sea ice experts, we were able to identify the most locally relevant processes influencing fracture formation and prioritize them in our analysis. We highlight that the dominant processes governing fracture formation in Admiralty Inlet and other constrained waterways of the Canadian Arctic Archipelago are different from the dominant processes governing fracture in pack ice or in landfast ice exposed to the open ocean (e.g., north shore of Alaska, the Eastern Siberian Sea, and the Kara Sea).

4 Data

4.1 Fracture dataset

We used the fracture locations identified in Admiralty Inlet, Nunavut using Sentinel-1 interferometric synthetic aperture radar (InSAR) from December to May and Sentinel-2 true-colour imagery from May to July in 2018 to 2023 described in detail in Loewen et al. (2026) (Figure 2). Fractures were identified manually in each image and some were validated using *in-situ* observations and Inuit Knowledge of the locations of fractures in this region. Each fracture feature was assigned a 'FractureID' attribute for each year that allowed fractures occurring in approximately the same location be tracked throughout the year using the same 'FractureID'.

In InSAR interferograms, fractures are indicated by discontinuities in the interferometric phase caused by differential changes in ice deformation in the along-track direction on each side of a fracture between image acquisitions (12 days). If a fracture is open, but there is no differential motion in the along-track direction on each side of the fracture, it cannot be identified using this method. In April and May, the coherence of InSAR interferograms can decrease due to changes in surface scatterers, making it more difficult to observe fractures. This can artificially lower the number of fractures that can be observed, especially near the shorelines, which experience surface melting earlier than in the middle of the inlet.

Fractures can be identified in Sentinel-2 through differences in surface reflectance properties in the pixels surrounding fractures (e.g., dark-coloured pixels indicating open water surrounded by white/blue pixels indicating sea ice). Sentinel-2 imagery were available approximately daily, but not all fractures could be identified in all images due to snow covering the ice surface or cloud cover over the scene.

Fracture widths could not be estimated from these satellite images, but the minimum width of fractures that can be identified from InSAR is less than a millimetre (Fedders et al., 2025), which is far below the scale that is relevant to community members, and approximately 10 m from Sentinel-2. We filtered out 'FractureIDs' that were observed for less than 14 days to limit the number of spurious features in this analysis.

https://doi.org/10.5194/egusphere-2026-3739
Preprint. Discussion started: 2 July 2026

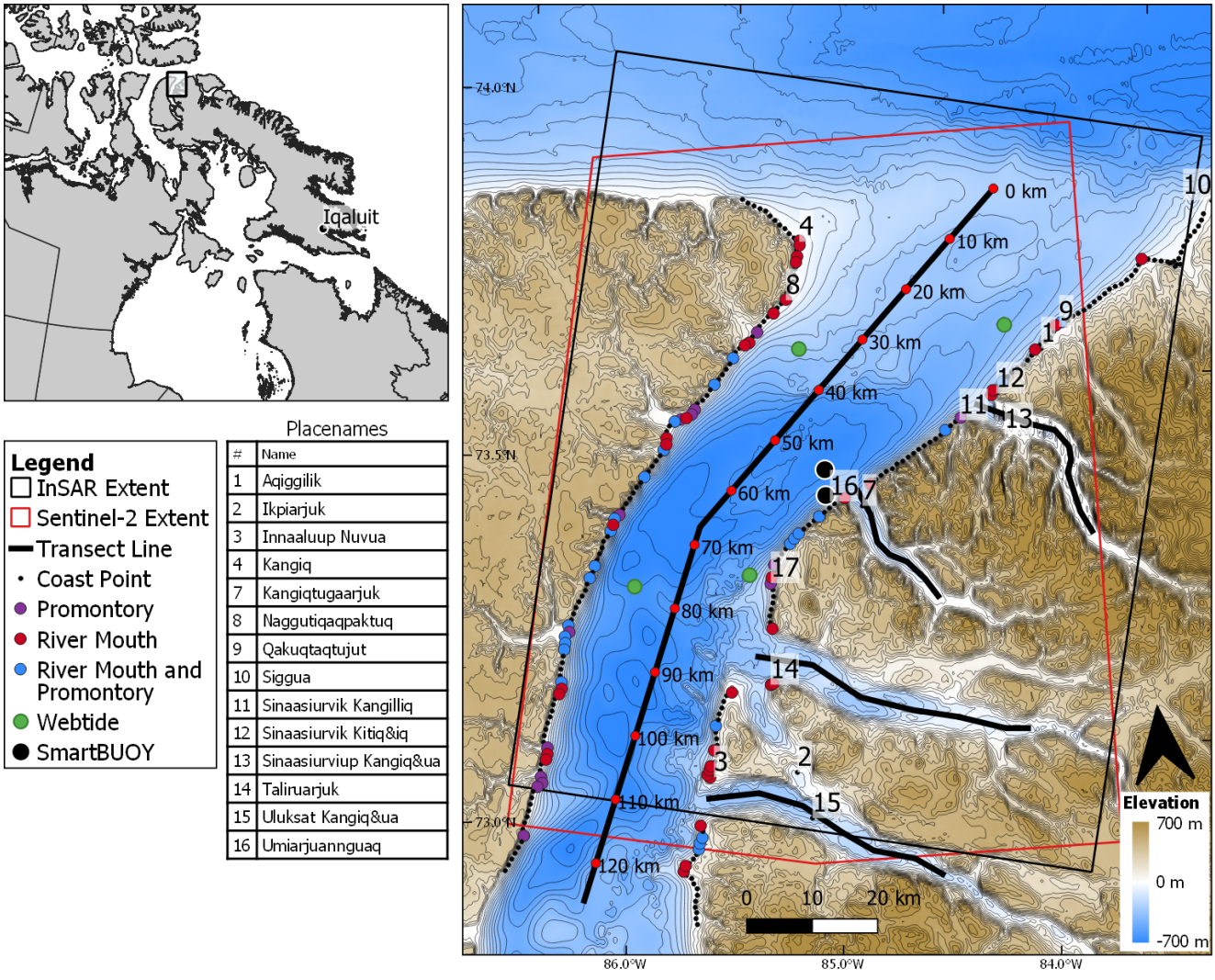

Placenames

#	Name
1	Aqiggilik
2	Ikpiarjuk
3	Innaaluup Nuvua
4	Kangiq
7	Kangiqtugaarjuk
8	Naggutiqaqpaktuq
9	Qakuqtaqtujut
10	Siggua
11	Sinaasiurvik Kangilliq
12	Sinaasiurvik Kitiq&iq
13	Sinaasiurviup Kangiq&ua
14	Taliruarjuk
15	Uluksat Kangiq&ua
16	Umiarjuannguaq

Figure 2. InSAR and Sentinel-2 image extents, locations of points of land (promontory point) and river mouths, and transect lines that were used for analysis of fracture patterns. SmartBUOY deployment locations and Webtide points used for environmental data analysis are also noted.

https://doi.org/10.5194/egusphere-2026-3739
Preprint. Discussion started: 2 July 2026

4.2 Environmental data

Long-term *in-situ* weather information in Arctic regions is usually limited to sparsely distributed community airports, which can have data outages due to hardware issues. The nearest currently operating long-term weather station to Admiralty Inlet is found at the Arctic Bay airport (CXAT) in the adjacent Adams Sound. Wind speed and direction from this station are not representative of winds in Admiralty Inlet due to the topography of the area (Loewen et al., 2025). Instead, we use 2 air temperature, U, and V wind components from ERA5 (Hersbach et al., 2025) at a grid cell near the floe edge in Admiralty Inlet. ERA5 underestimates wind speeds in Admiralty Inlet, but are more closely correlated with observed wind speeds from a short-term weather station located in the inlet than winds from CXAT (Loewen et al., 2025).

Ocean current observations in Admiralty Inlet are scarce, but the European Union Copernicus Marine Service Information Global Ocean Physics Reanalysis product (E.U. Copernicus Marine Service Information (CMEMS). Marine Data Store (MDS)., 2024) indicated 6-hour and daily averaged mean flows were on the order of 1 cm/s for this region. Ocean currents up to 90 cm/s have been observed near the mouth of the inlet at Kangiq (Cape Crawford; Point 4 in Figure 2) where there is flow into Admiralty Inlet from Lancaster Sound (Fissel and Wilton, 1978). Therefore, we conclude that non-tidal currents are irrelevant to fracture processes at the regional scale, but may be important locally. Instead, we use 15 min tidal currents modelled by the Bedford Institute of Oceanography's WebTide Arctic model (Collins et al., 2011) which on the order of 10 cm/s to 20 cm/s at four locations chosen throughout Admiralty Inlet (Figure 2).

SmartICE collects ice thickness and temperature data around Ikpiarjuk, Nunavut in collaboration with Arctic Bay Adventures, a local outfitting company. The SmartQAMUTIK is a Geonics Ltd., EM-31 sensor enclosed in a wooden box on a qamutik, a traditional Inuit sled, pulled by a snowmobile which measures the combined snow and ice thickness as the snowmobile drives. The locations and timing of SmartQAMUTIK runs are determined by community needs and priorities and extend throughout Admiralty Inlet and its side inlets. We used SmartQAMUTIK data collected around Ikpiarjuk from January to June from 2018 to 2023 to estimate monthly ice thicknesses in this region. Snow depths in Admiralty Inlet range from 0 cm to 40 cm, increasing approximately linearly to maximum snow depth in April or May and decreasing back to 0 cm by mid-June (Canadian Ice Service, 2024). Snow thickness was not removed from SmartQAMUTIK measurements.

The SmartBUOY is a thermistor chain frozen into the sea ice that measures ice temperature profiles at 4 cm intervals every 12 hours. SmartBUOYs were deployed February to May 2021 and March to June in 2022 near Umiarjuannguaq (Figure 2, Point 16). We use SmartBUOY data to calculate average ice temperatures for each month that data were available.

4.3 Geographical datasets

Shoreline geometry data were derived from a modified shapefile of Canada's major landmasses and coastal areas from Stats Canada (Statistics Canada, 2016), using Planet images (Planet Labs) as a basemap to manually improve the accuracy of the shoreline in Admiralty Inlet. We resampled this dataset to create a set of shoreline points every 100 for our area of interest. The International Bathymetric Chart of the Arctic Ocean (IBCAO) Version 4.0 was used for bathymetry data of the region (Jakobsson et al., 2020).

https://doi.org/10.5194/egusphere-2026-3739
Preprint. Discussion started: 2 July 2026

5 Methods

5.1 Spatial and temporal patterns of fracture density

We generated heatmaps of the spatial distribution of all fractures within each year (yearly heatmaps) and for fractures across all years for each month (monthly heatmaps). To do this, we first rasterized each fracture polyline onto a 1 km x 1 km grid for each unique observation date (or date range, in the case of InSAR), generating binary raster layers indicating fracture presence or absence in each cell. Although 1 km is coarse and fractures that reform in similar locations may get merged into the same grid cell, this resolution is sufficient for qualitative identification of recurring fracture zones. Detailed analysis of individual fracture lifetimes are described separately in Section 5.2.3.

For each analysis period (yearly, monthly), we then calculated the average fracture occurrence frequency in each grid cell by summing the binary values across all images in the interval and dividing by the total number of images for that period. The resulting values represent the mean frequency of fracture appearance in each cell over the specified time range. In addition, we converted the yearly heatmaps into binary heatmaps (i.e., cells with average fracture occurrence > 0 were assigned a value of 1) and summed these binary heatmaps to show the total number of years in which a fracture occurred at each location within the area of interest, regardless of the frequency of appearance within any particular year.

To examine spatial and temporal variability in fracture appearance, we extracted fracture occurrence frequency from the heatmaps for each month of each year along a north-south transect approximately centred within the inlet (Figure 2). We also extracted values from the yearly heatmaps along the same north-south transect in Admiralty Inlet, as well as along additional transects placed through the centres of each side inlet to estimate the spacing of fractures in each of these inlets (Figure 2). The local maxima in fracture occurrence frequency along each transect correspond to zones of concentrated fracturing throughout each year, which we identified and used to calculate the distances between successive maxima.

5.2 Vector-based feature classification

The previous section described a method to rasterize fracture location data for identifying broad spatial and temporal trends in fracture formation. Here, we present methods that analyze spatial and temporal fracture patterns using the vector-based fracture dataset.

5.2.1 Spatial categorization of fractures

We calculated the distance between each fracture endpoint and the nearest shoreline point or shoreline point that was deemed to be near a promontory, and categorized each fracture feature by their distance from the shoreline. Fractures were classified as ‘long’ if both endpoints were within 5 km of a shoreline point; all others were classified as ‘short’. Short fractures were further categorized based on which shoreline, if any, they were associated with. Fractures whose eastern endpoint was within 5 km of the east shoreline and western endpoint was more than 5 km away from the west shoreline were classified as east-shore

https://doi.org/10.5194/egusphere-2026-3739
Preprint. Discussion started: 2 July 2026

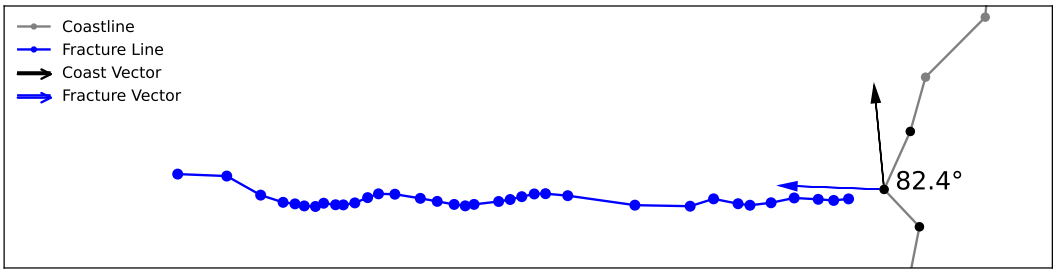

Figure 3. Example of a fracture vector relative to a shoreline vector for calculating fracture angles.

fractures. West-shore fractures were classified in the same way but in reverse. Short fractures for which both endpoints were more than 5 km from any shoreline point were classified as not associated with either shore.

5.2.2 Geometric properties of fractures

For each fracture feature, we calculated the angle (θ) between the closest segment of each fracture vector and the nearest segment of the shoreline. To do this, first, we identified the two end points of the fracture and used these points to construct a vector representing the fracture orientation ($\boldsymbol{f}$). We then extended this vector toward the shoreline to determine its intersection point. Using the three shoreline points nearest to this intersection, we constructed a second vector representing the local shoreline orientation ($\boldsymbol{s}$). To maintain a consistent sign convention, fracture vectors were towards the east or to the west depending on the shore to which they were referenced, and shoreline vectors to the north. The angle between the two vectors was then computed as

$$\theta = acos\left(\frac{\boldsymbol{f}\cdot\boldsymbol{s}}{|\boldsymbol{f}||\boldsymbol{s}|}\right). \quad (4)$$

90° angles indicate fractures perpendicular to the shoreline. Angles less than 90° represent fractures that slope positively (north of perpendicular), whereas angles greater than 90° indicate fractures that slope negatively (south of perpendicular).

Fracture sinuosity was calculated as the ratio of the straight-line distance between fracture endpoints to the total length for each fracture. Values approaching 1 indicate nearly straight fractures, while lower values indicate fractures with greater curvature. For each fracture category, we computed the mean and standard deviation values for angle and sinuosity.

5.2.3 Temporal categorization of fractures

We extracted the first and last dates that each unique 'FractureID' value was observed in a given year to determine the month it first appeared and to estimate how long it persisted during the ice season. In addition, we identified the fracture category at both the first and last observation of each 'FractureID' and counted the number of fractures corresponding to each combination of initial and final categories to assess how fractures evolved over time.

https://doi.org/10.5194/egusphere-2026-3739
Preprint. Discussion started: 2 July 2026

We do not attempt to quantify whether fractures open and close throughout the year, as fracture observations may have been missed due to a lack of deformation preventing observation (for InSAR), or the fracture width being too small for detection (primarily for true-colour imagery). Despite these limitations, this dataset does reveal broad patterns of fracture evolution across the study area.

5.2.4 Spatial correlation with shoreline features

We quantified the relationship between fracture locations and 'special' shoreline points (promontory points, inlet mouths, and river mouths). Promontory points, secondary inlet mouths, and river mouths were manually identified on the shoreline geometry polyline vector described in Section 4.2 using Sentinel-2 imagery as a basemap. For each shoreline point, we calculated the sum of the inverse distances between that point and the nearest endpoint of every fracture in each fracture length category. Then, for each category of 'special' shoreline points, we performed a Mann-Whitney U test to determine whether the sum of the inverse distance values differed significantly in each 'special' point category from those of 'normal' shoreline points (Denis, 2021). We use this non-parametric test because not all the sum of the inverse distance distributions were normally distributed. We conducted separate tests for each fracture length category and for the east and west shores. The U statistic was used to calculate the common language effect size ($f = \frac{U}{n_1 n_2}$), which indicates the probability that a randomly selected value from one group (e.g., sum of fracture distances to a promontory point) will be greater than a randomly selected value from the other group (e.g., sum of fracture distances to any shoreline point) (Kerby, 2014).

5.3 Evaluating potential drivers for fracture formation

As outlined in Section 2, two main factors affect fracture formation: ice strength and external forces acting on the ice cover. We hypothesize that seasonal changes in ice properties and environmental forcing influence the timing of fracture formation, while shoreline geometry concentrates stress in specific locations, causing fractures to form in recurring locations. To evaluate these hypotheses, we (1) make first-order estimates of the magnitude and seasonal changes in ice strength and external stresses (thermal, wind, and current) on sea ice based on environmental data that are available for Admiralty Inlet, and (2) quantify the relationship between fracture formation locations and promontory points and river mouths, which are known to have the potential to concentrate stresses.

5.3.1 Ice strength

We apply Timco and Weeks's (2010) equation for tensile strength (σ_t; MPa) for first-year ice (Equation 5) to qualitatively estimate how ice strength in Admiralty Inlet changes throughout the ice season:

$$\sigma_t = 4.278\, v_T^{-0.6455}. \tag{5}$$

Total brine volume (v_T) is the sum of the brine volume (v_b; ppt) and air volume. We assume air volume is zero, although this assumption may not be accurate in the spring as brine channels drain. We estimate brine volume from Timco and Weeks

https://doi.org/10.5194/egusphere-2026-3739
Preprint. Discussion started: 2 July 2026

(2010) (Equation 6), which is dependent on ice temperature (T_i; °C) and ice salinity (S_i; ppt). Ice salinity is estimated from ice thickness (h_i), as in Equation 7 (Timco and Weeks, 2010).

$$\nu_b = S_i \left[\frac{49.185}{|T_i|} + 0.532 \right] \tag{6}$$

$$S_i = 4.606 + \left[\frac{91.603}{h_i} \right] \tag{7}$$

Other computed measures of ice strength (e.g. flexural) would show similar seasonal patterns. Equation 5 is an empirical relationship derived from laboratory experiments, so the magnitudes are not appropriate for sea ice strength at geophysical scales, which is on the order of 10s of kPa (Richter-Menge and Elder, 1998; Tucker and Perovich, 1992; Plante et al., 2020). Instead, we normalize the calculated ice strength values by the maximum ice strength value to examine the relative change in ice strength throughout the ice season.

We use SmartBUOY data to estimate mean ice temperatures from January to June and SmartQAMUTIK data to estimate mean ice thicknesses in Admiralty Inlet from January to June to then calculate ice salinity and brine volume. Since SmartBUOY and SmartQAMUTIK data were not available in December, we average December ice thickness data collected in Admiralty Inlet from 1959 to 1966 and in 1970 from the Canadian Ice Service Ice Thickness Program, which was approximately 72 cm (Canadian Ice Service, 2024). We assume ice temperatures are at the freezing point (-1.8 °C) in December, although this is likely an overestimate of ice temperatures during this month. Varying ice temperatures in December between -1.8 °C and -6 °C do not qualitatively change our results of seasonal patterns of ice strength.

5.3.2 Thermal stress index

To make a first-order approximation of thermal stresses in sea ice for each year from 2018 to 2023, we calculate daily average temperature differences from ERA5 2 air temperatures from December to July. In reality, additional processes influence the magnitude of thermal stresses in sea ice. Surface ice temperatures (0-10 cm) primarily determine thermal stresses in ice, which are affected by snow cover insulating effects and upper and lower ice surface energy fluxes (Kaidel et al., 2025). In addition, thermal stress can dissipate slowly over time, leading to the accumulation of residual stresses after repeated cooling and warming cycles (Hata and Tremblay, 2015). Land confinement may also cause directional differences in stress magnitudes as the ice is either allowed or prevented from deforming in certain directions (Hata and Tremblay, 2015; Teigen et al., 2005). Little data are available to constrain the impact of these processes in Admiralty Inlet.

5.3.3 Environmental stresses

To estimate the first-order effect of wind and ocean current stresses on internal stresses within landfast ice, we use the one-dimensional model of a sheet of landfast ice of length *L* anchored to the shore on one side (i.e., no motion at the fixed end) described by König Beatty and Holland (2010):

https://doi.org/10.5194/egusphere-2026-3739
Preprint. Discussion started: 2 July 2026

Table 1. Constants used for wind and current stress calculations.

Variable name	Variable	Value	Unit	Reference
Wind drag coefficient	c_a	0.001	-	König Beatty and Holland (2010)
Ocean drag coefficient	c_w	0.004	-	König Beatty and Holland (2010)
Air density	ρ_a	1.3	kg m^{-3}	König Beatty and Holland (2010)
Ocean density	ρ_w	1025	kg m^{-3}	König Beatty and Holland (2010)

$$\sigma(x) = \tau_i(L - x) \tag{8}$$

where σ is the ice stress which varies along the length of the ice sheet, L is the maximum length the ice, and x is the position along the ice sheet from the shore. The maximum internal stress magnitude occurs at the shore (x = 0). We can estimate the maximum ice length that can be supported by assuming that the stress at the shore equals the tensile strength of the ice (T):

$$L_{max} = \frac{T}{\tau_k}. \tag{9}$$

We assume a spatially and temporally constant offshore wind or current stress (τ_k, where k is a for wind stresses or o for current stresses) given by Equation 2 using constants in Table 1. Wind and current drag coefficients change with surface roughness and atmospheric/oceanic stability (Tsamados et al., 2014). Wind drag coefficients for first year ice range from 1.0 x 10^{-3} to 1.5 x 10^{-3} (Mchedlishvili et al., 2023), and current drag coefficients can range from 1.0 x 10^{-3} to 22.3 x 10^{-3}, with lower values (<7.3 x 10^{-3}) corresponding to landfast ice (Lu et al., 2011).

This simple model assumes the ice is confined on one end and unconfined on its sides, which is a valid assumption for Admiralty Inlet only in the late spring if shoreline melting has caused the ice to become unfastened from the shore (Loewen et al., 2025). We do not attempt to model the effect of confined edges analytically, but note that adding this effect would increase the strength parameter of the ice. Thus, we use the results from this model to estimate the minimum wind and currents stresses required to cause fracture.

6 Results

6.1 Spatial and temporal patterns of fracture formation

6.1.1 Yearly and monthly fracture patterns

Several patterns were observed from yearly heatmaps of fractures formed in each year from 2018 to 2023: (1) fractures occurred generally all over Admiralty Inlet (Figure 4a), but (2) there were certain zones where fractures formed more frequently than others, and (3) there was interannual variability in the locations and number of fractures observed in each year (Figure 4b-g).

https://doi.org/10.5194/egusphere-2026-3739
Preprint. Discussion started: 2 July 2026

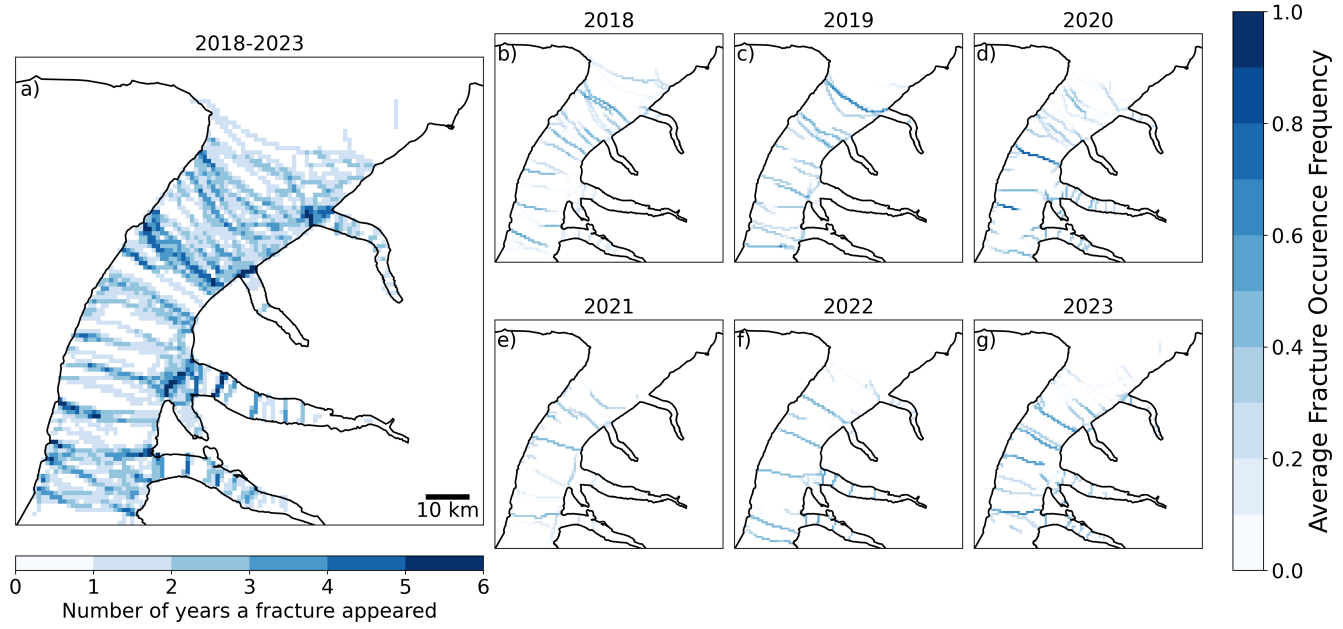

Figure 4. Locations of all fractures in each year from 2018 to 2023. Darker colours indicate greater likelihood of fracture appearance. Note the 2018-2023 heatmap (a) indicates the number of years each pixel had a fracture observed over the six-year period (regardless of the frequency of observation in each year), whereas the yearly heatmaps (b-g) indicate the frequency of observations of fractures in each pixel within the year.

The spread of zones of recurring fractures were generally narrower in the secondary fiords that extend away from Admiralty Inlet than within Admiralty Inlet itself (Figure 4a).

Some fractures were short-lived while others appeared intermittently throughout the season (Figures 5 and 6). Fractures that persisted for much of the season tended to occur in the same locations where fractures repeatedly formed across multiple years, suggesting consistent zones of concentrated stress within the landfast ice cover (Figure 6).

6.1.2 Fracture spacing

Although fracture spacing along the central Admiralty Inlet transect varied widely, distance intervals of 2-4 km, 7-11 km, and 18-19 km between fractures occurred most frequently across all years examined (Figure 7). Peak distances between fractures in the secondary inlets clustered primarily within the 2-8 km range, with no prominent peaks at distances greater than 10 km (Figure 7, inset). Admiralty Inlet is approximately 25 km to 40 km wide, while the secondary inlets are approximately 4 km to 7 km wide, corresponding to roughly 10% to 30% of the width of the main inlet. This proportionality is approximately consistent with the smaller fracture spacing observed in the secondary inlets (2-8 km) compared to Admiralty Inlet (7-11 km, 18-19 km).

https://doi.org/10.5194/egusphere-2026-3739
Preprint. Discussion started: 2 July 2026

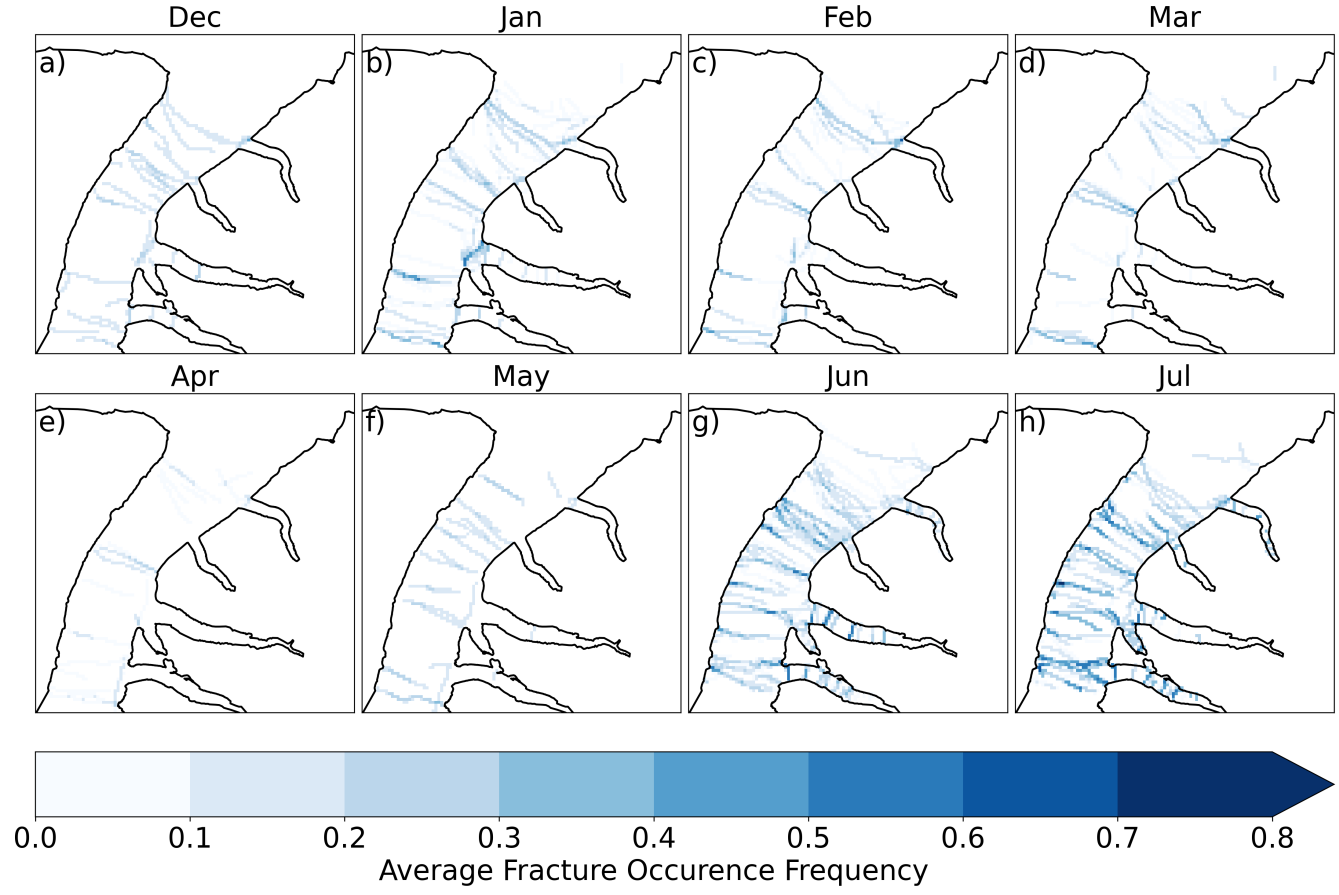

Figure 5. Average fracture occurrence frequency of all fractures in each month for all years (2018 to 2023). Darker colours indicate greater likelihood of fracture appearance.

6.1.3 Fracture categorization and geometric properties

Most fractures extended partially across the inlet (79%) ('short fractures'), as opposed to fully across the inlet (21%) ('long fractures') (Figure 8). Of the fractures that extended only partially across the inlet, the majority of them extended from either the east shore (46.3%) or west shore (47.0%), while few started and ended in the middle of the inlet (6.7%) (Table 2). The locations of long fractures tended to concentrate in certain zones within Admiralty Inlet, and generally matched the locations of recurring fractures (Figures 4, 8a). In contrast, short fracture locations did not appear to be as spatially consistent (Figure 8b).

The sinuosity of all fracture types ranged from 0.93 to 0.96, which means that they had relatively straight geometries (Table 2). On average, all fracture types formed angles approximately perpendicular to the shoreline (86° to 96°), with some variation within each category (Table 2).

https://doi.org/10.5194/egusphere-2026-3739
Preprint. Discussion started: 2 July 2026

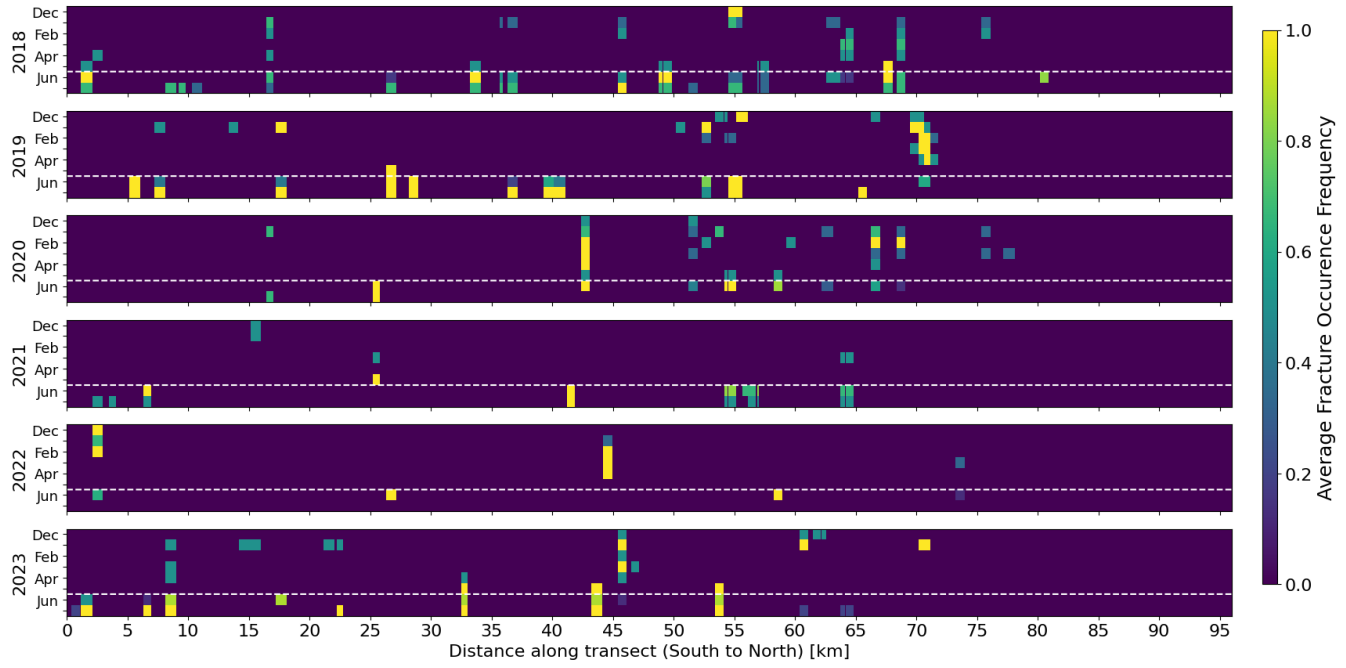

Figure 6. Transect of probability of fracture formation ('Average Fracture Occurrence Frequency') between December and July in each year from 2018 to 2023. Green and yellow areas are where fractures were more likely to form. Dark blue pixels are areas where no fractures formed. White horizontal lines indicate the transition from fractures identified by InSAR to fracture identified in Sentinel-2 true colour images.

Table 2. Geometric characteristics of different fracture length categories. 'Long' fractures extend across Admiralty Inlet. 'Short' fractures extend partially across and terminate near the east shore, west shore, or neither shore. θ is the mean fracture angle ($\pm$ standard deviation) relative to the nearest shoreline segment. Sinuosity is the ratio of the straight-line endpoint distance to total fracture length (mean $\pm$ standard deviation). Proportion is the number of fractures in each category divided by the total; values in parentheses show the percentage breakdown of short fracture subcategories. N/A indicates not available.

Fracture Type	θ (East Shore) (°)	θ (West Shore) (°)	Sinuosity	Proportion (%)
Long	92.4 ± 14.9	86.6 ± 9.6	0.9588 ± 0.062	20.9
Short (neither)	N/A	N/A	0.9562 ± 0.127	5.3 (6.7)
Short (East)	105.7 ± 29.7	N/A	0.9309 ± 0.149	36.6 (46.3)
Short (West)	N/A	87.0 ± 20.2	0.9605 ± 0.0938	37.2 (47.0)

https://doi.org/10.5194/egusphere-2026-3739
Preprint. Discussion started: 2 July 2026

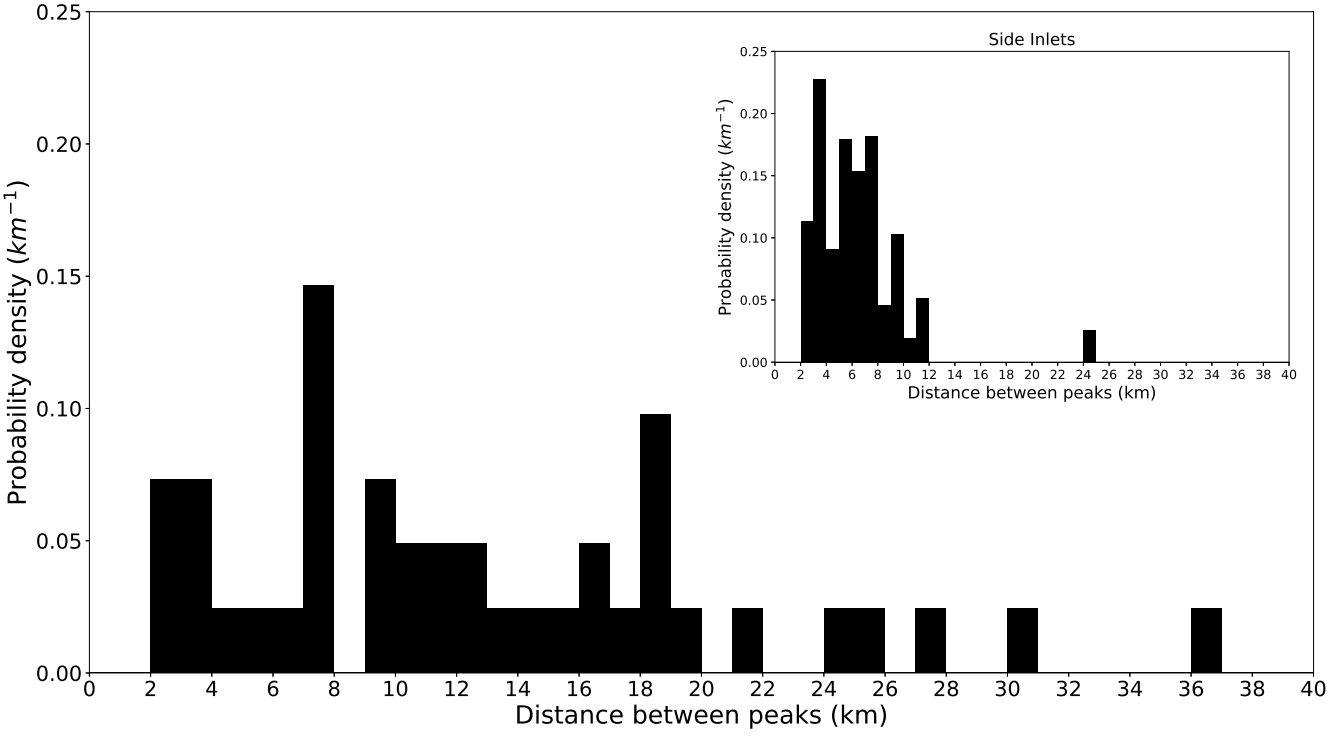

Figure 7. Histogram of distances between peaks of fracture heatmap probabilities along the central transect in Admiralty Inlet (main axis) and its side inlets (inset) for all years.

6.1.4 Seasonal patterns in fracture formation

Fracture initiation across all length categories most commonly occurred in December and January as the ice froze and consolidated (Figure 9a). Fracture formation reduced from February to May, but many new fractures appeared in June, primarily due to the formation of short fractures extending from both shores (not shown). Fractures originating from the east shore tended to form in both early winter (47% in December/January) and late spring (40% in June), while fractures originating from the west shore tended to form only in the late spring (59% formed in June/July). Although ice breakup in early to mid-July means that fewer satellite images were used to identify fractures in this month compared to other months, July still showed the second-highest number of observed fractures, most of which formed earlier in the season and included a mix of all fracture length types.

Physically, fractures may refreeze and remain closed, reopen later in the season, or stay open continuously throughout the winter and spring. Once fractures opened, they generally followed one of two patterns: remained open for periods typically shorter than 90 days (for fractures forming in December and January) or opened and remained open for the remainder of the ice season (Figure 9b). Fractures that formed in June almost always persisted through to breakup. We cannot track fractures that open, close, and later re-open in this dataset.

https://doi.org/10.5194/egusphere-2026-3739
Preprint. Discussion started: 2 July 2026

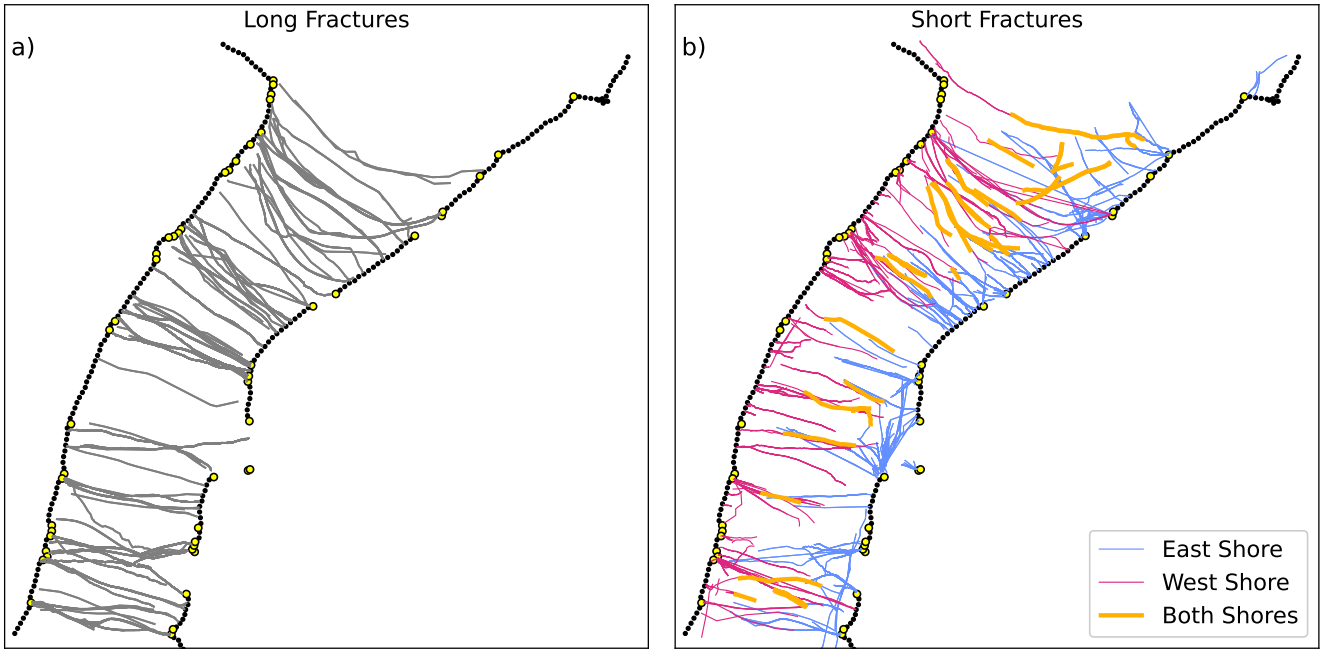

Figure 8. Spatial distributions of different fracture length categories for all years. (a) Long fractures that extend across Admiralty Inlet (both end points $<$ 5 km from shore). (b) Short fractures that extend only partially across Admiralty Inlet, starting from the west shore (pink), east shore (blue), or starting and ending away from both shores (orange). Shoreline points are shown in black and yellow. Yellow shoreline points indicate promontories or inlet mouths.

6.1.5 Direction of fracture growth

Fractures generally remained within the same length category from their first appearance to their final observation in satellite imagery (Table 2). Long fractures typically began as long features or originated along the west shore and later lengthened. In contrast, few east shore fractures reached long lengths, and none that formed in the middle of the inlet did so. Short fractures that did not initially reach either shore generally stayed within their original length category, except for those that later extended toward the east shore.

Fractures that first appeared long and later categorized as short near neither shore may have shortened due to physical processes, such as partial refreezing, although reduced coherence nearshore or cloud contamination in imagery could also explain this pattern by limiting the image area available for fracture identification. Short fractures that appeared to switch shores may have temporarily grown into long fractures that reached the opposite shoreline before refreezing from their original side. Alternatively, these cases may reflect misclassification of edge cases.

https://doi.org/10.5194/egusphere-2026-3739
Preprint. Discussion started: 2 July 2026

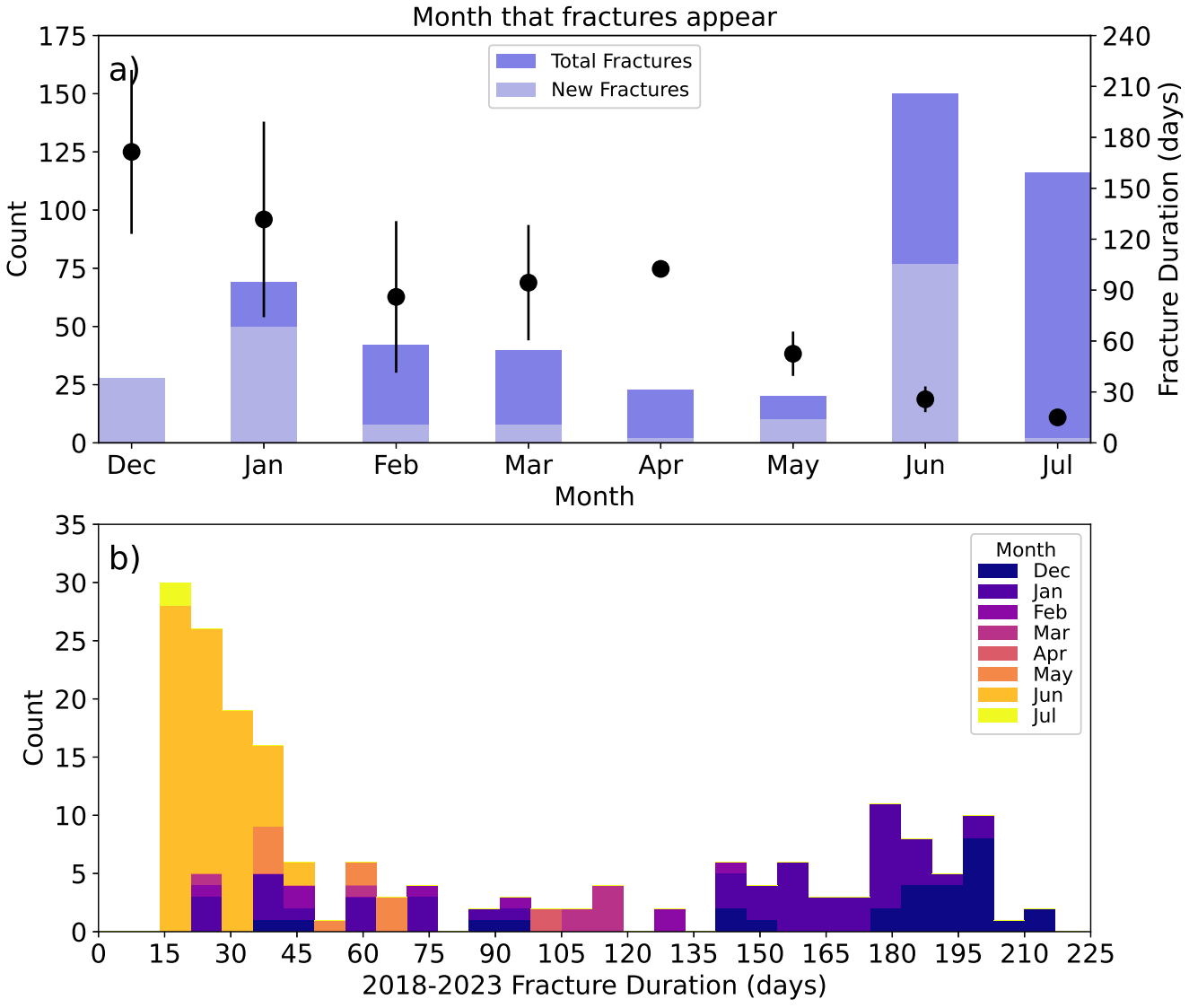

Figure 9. Seasonal patterns in fracture formation and duration. (a) Number of new fractures appearing in each month (bar lines) plotted against the time duration of each of these fractures (time duration defined as the time between the first and last observation of a fracture with the same 'Fracture ID' attribute) (points with error markers). (b) Histogram of fracture duration in days for all fractures from 2018-2023. Colours indicate the month fractures first appeared.

https://doi.org/10.5194/egusphere-2026-3739
Preprint. Discussion started: 2 July 2026

Table 3. Number of fractures starting and ending in each fracture category for all years in count and percent. Bolded rows indicate end categories that match the initial category.

Initial Category	End Category	Count	Percent (per initial category)
Long	**Long**	**14**	**58%**
	Short (east)	3	13%
	Short (west)	7	29%
Short (neither)	**Short (neither)**	**8**	**50%**
	Short (east)	8	50%
Short (east)	Long	4	5%
	Short (neither)	2	3%
	Short (east)	**64**	**84%**
	Short (west)	6	8%
Short (west)	Long	10	14%
	Short (neither)	2	3%
	Short (east)	2	3%
	Short (west)	**57**	**80%**

6.2 Potential drivers of fracture formation

6.2.1 Ice strength

Calculated normalized ice strength increased to a maximum in March and decreased to a minimum by June (Figure 10a) which is consistent with borehole strength measurements of first-year ice in the spring (Johnston, 2017). Intuitively, as ice thickness increases throughout the ice season, we expect ice strength to increase until the ice begins to warm and brine pockets expand, changing the microstructure of the ice (Maus, 2023). Ikpiarjukmiut have observed that, as maximum spring ice thicknesses have decreased in Admiralty Inlet in recent decades, more fractures have formed than in previous decades when ice was thicker (SmartICE, 2022).

6.2.2 Thermal stress index

Monthly average air temperatures were lowest in December to March (-25 °C to -30 °C), then gradually increased to above 0 °C by June and July, with some interannual variability (Figure 11a). The relative magnitude of average warming versus cooling events for all months was approximately the same (Figure 11b). The strongest cooling events occurred in December and February to April, while the strongest warming events occurred from December to April. Warming events indicate compressive stresses due to thermal expansion, while cooling events indicate tensile stresses due to thermal compression, although the magnitude of ice contraction and expansion is highly ice temperature dependent (Kaidel et al., 2025). The thermal expansion coefficient is negligible once upper (0-10 cm) ice temperatures exceed -11 °C (Kaidel et al., 2025).

https://doi.org/10.5194/egusphere-2026-3739
Preprint. Discussion started: 2 July 2026

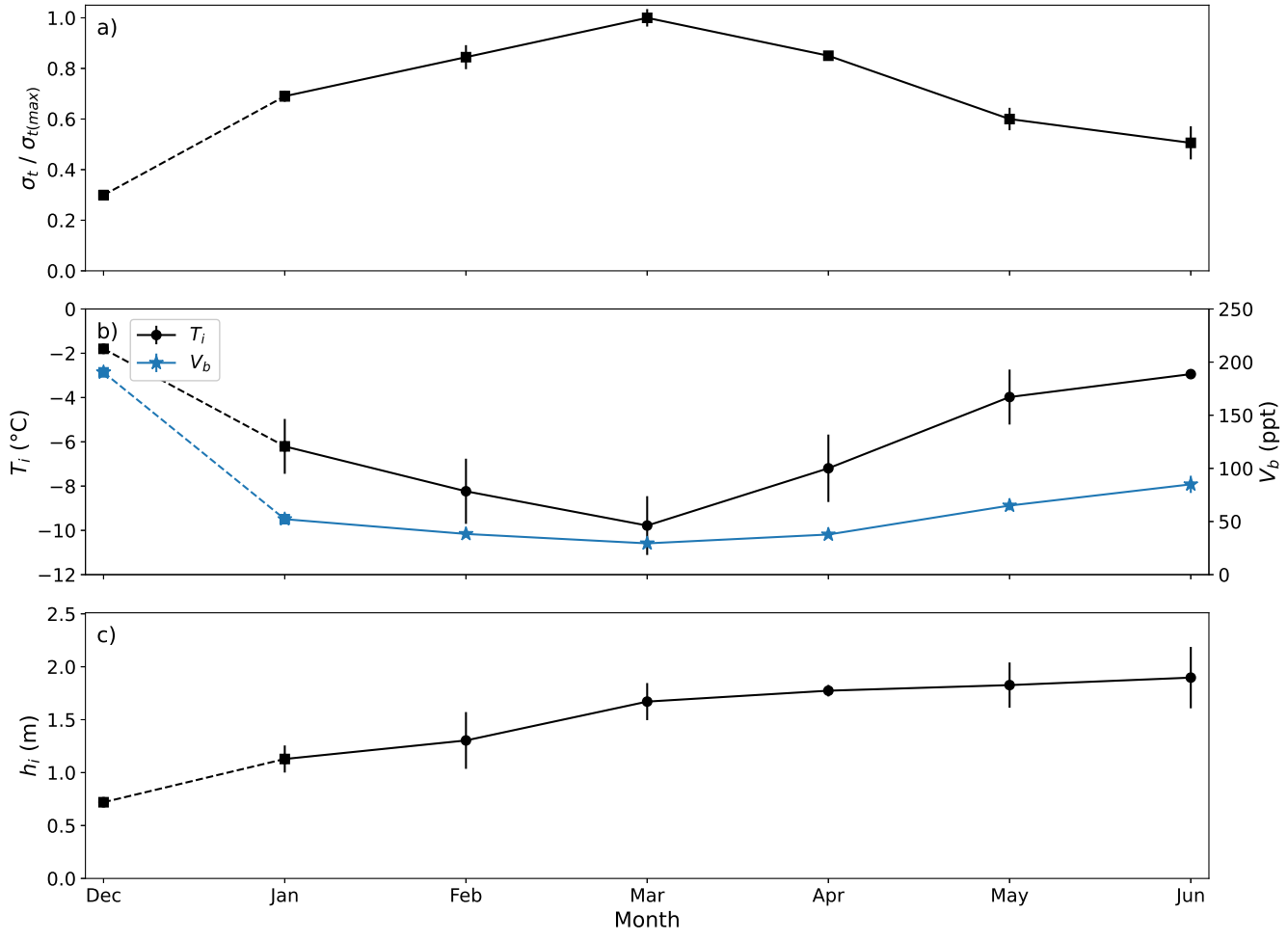

Figure 10. Measured and calculated ice properties throughout the ice season. (a) Scaled (black) and normalized (blue) values for the calculated tensile strength of sea ice for each month from January to June. (b) Monthly averaged near-surface ice temperatures (T_i; black) from SmartBUOY data and calculated brine values (ν_v; blue). (c) Monthly averaged ice thicknesses (h_i) from SmartQAMUTIK data. SmartBUOY and SmartQamutik data are not available for December, so T_i is assumed at -1.8 °C and h_i is assumed at 0.72 m in this month.

https://doi.org/10.5194/egusphere-2026-3739
Preprint. Discussion started: 2 July 2026

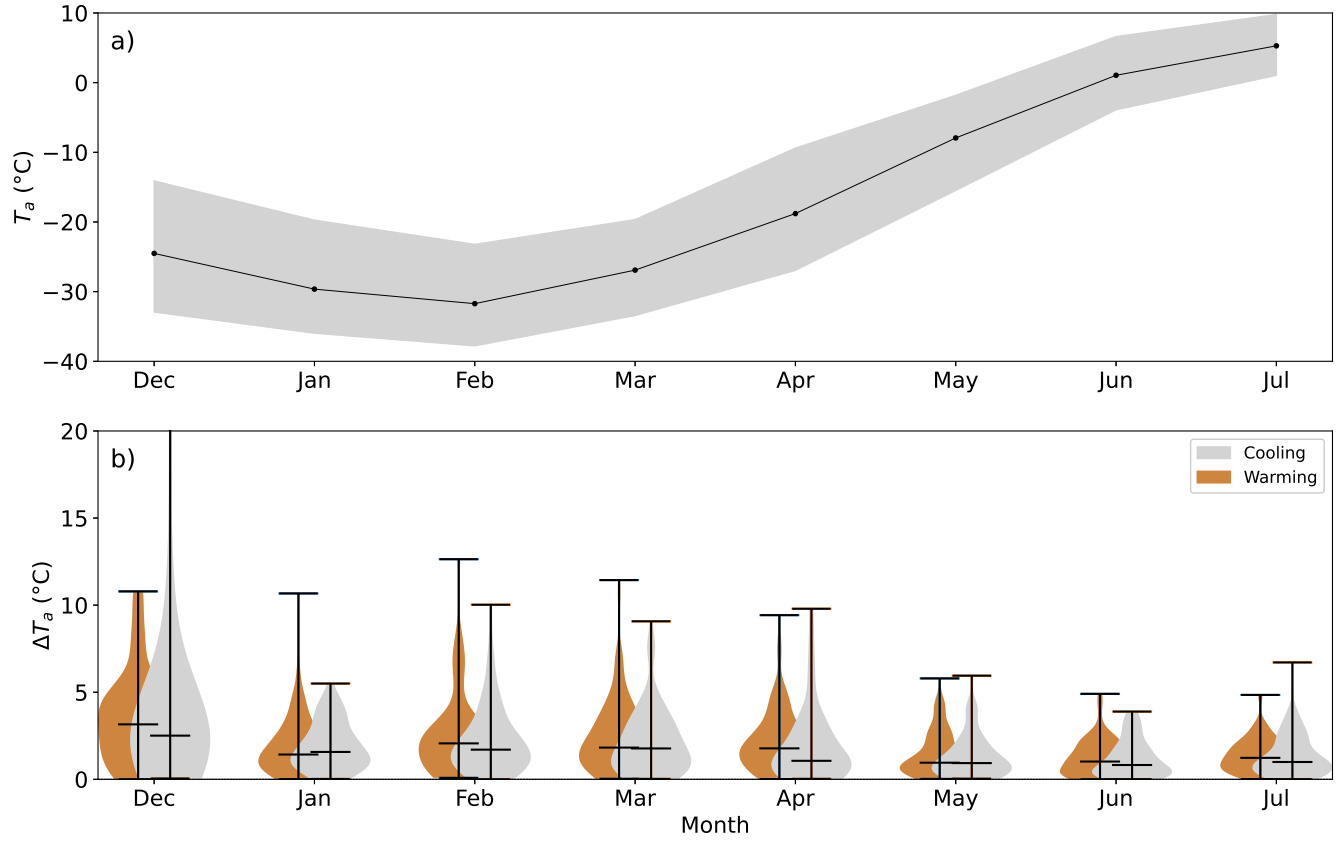

Figure 11. Monthly average air temperatures and daily temperature differences from 2018-2023. (a) Average ERA5 air temperatures (T_a). Grey shaded area indicates 5% to 95% interquartile range of air temperature values. (b) Violin plots of differences in daily average temperatures for each month in all years from 2018-2023. Grey plots indicate cooling events, while tan plots indicate warming events. Maximum cooling value in December is 38 °C.

6.2.3 Environmental stresses

ERA5 daily average wind speeds in Admiralty Inlet across all months and years were approximately 11 km/h, with the strongest monthly average winds occurring in December and May, and the weakest average winds occurring January and June, although the monthly variability was low (Figure 12a). Episodic events with daily average wind speeds greater than 25 km/h occurred in all months except January and February, with interannual variability.

Surface tidal currents varied daily and bi-weekly with spring and neap tides, with maximum speeds approximately of 18 cm/s (Figure 12b). We do not expect much seasonal variability of ocean currents once an ice cover has formed as sea ice friction dampens currents amplitudes and prevents the formation of wind-driven currents (Timmermans and Marshall, 2020).

https://doi.org/10.5194/egusphere-2026-3739
Preprint. Discussion started: 2 July 2026

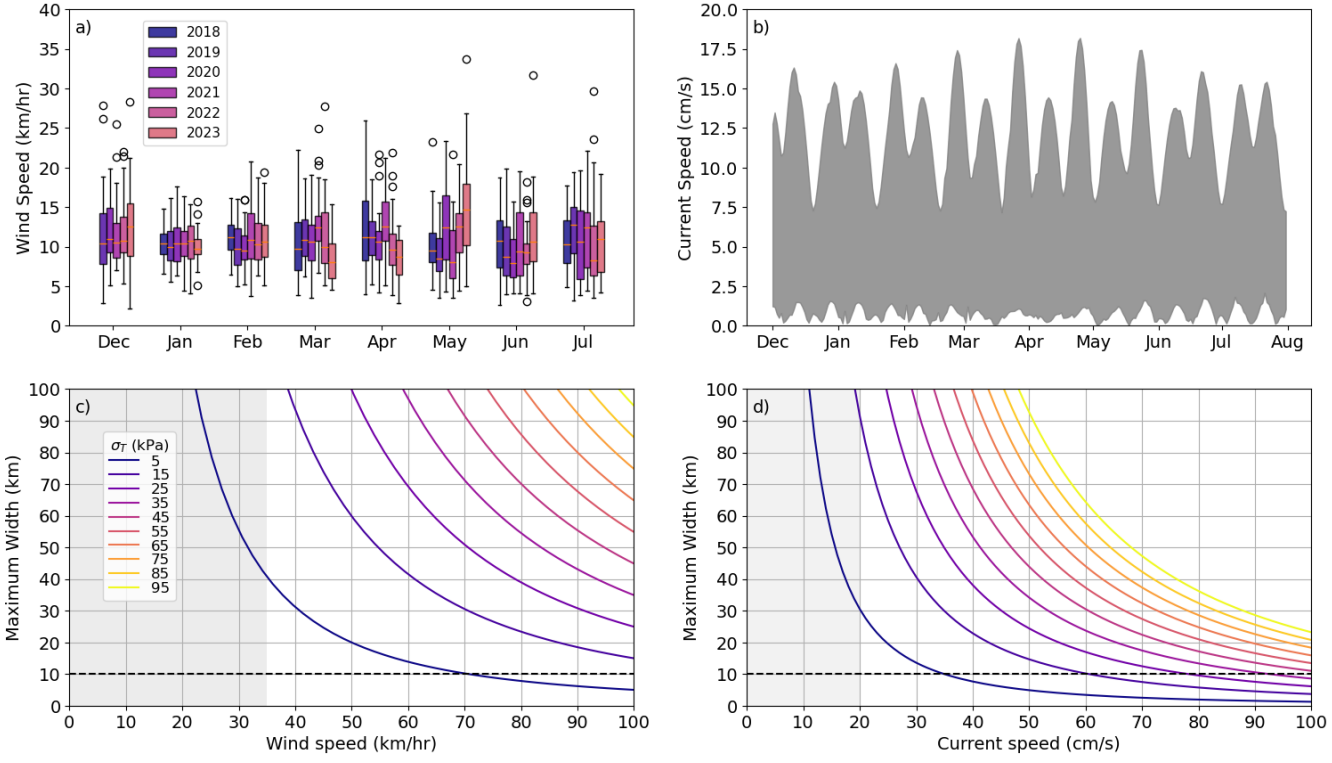

Figure 12. Monthly average wind and current speeds and model results using König Beatty and Holland's (2010) model. (a) Daily average ERA5 wind speeds per month, per year from 2018 to 2023, (b) Range of daily maximum and minimum tidal current speeds for a sample year from December to July, (c) Maximum length of landfast ice that can be supported by different wind speeds and tensile strength of ice, (d) Maximum length of landfast ice that can be supported by different current speeds and tensile strength of ice. Horizontal line in (c) and (d) indicates the wind/current speeds that would support a 10 km maximum landfast ice extent, the approximate distance between fracture in Admiralty Inlet and grey shaded area indicates the range of common wind/current values for Admiralty Inlet.

Our analysis of outputs from König Beatty and Holland's (2010) model shows that to produce a fracture spacing of 10 km in a landfast ice sheet, one mode of fracture spacing that we observed in Admiralty Inlet (Figure 7), would require either very strong winds (~75 km/h; 21 m/s) or strong currents (~32 cm/s) for a conservative tensile strength estimate of 5 kPa (Figure 12c, d). Wind speeds of this magnitude are uncommon, but not unheard of in the Arctic, and may increase in frequency in the future (Fox et al., 2023). Current speeds are not well constrained in Admiralty Inlet, but likely do not reach this magnitude except in locations with locally high current speeds (e.g., near the mouth of Admiralty Inlet; Fissel and Wilton, 1978).

Since wind and current stresses scale quadratically with speed (Equation 2), small changes in forcing can produce large differences in stress. Currents generate greater stresses than proportional wind speeds due to higher water density and drag (Figure 12d). Combining wind and current stresses would reduce the minimum wind speed required to produce fracture, which we do not illustrate here.

https://doi.org/10.5194/egusphere-2026-3739
Preprint. Discussion started: 2 July 2026

Table 4. Common language effect size and p-values (in brackets) from the Mann-Whitney U test for relationship between ends of fractures and promontory points, inlet mouths, and river mouths along the east and west shores ('_e' and '_w') for fractures that extend partially across the inlet ('short') and fractures that extend fully across the inlet ('long'). Bolded values indicate p-values < 0.05.

	short_e	short_w	long_e	long_w
Promontory Point	0.62 (0.0929)	**0.64 (0.0121)**	**0.72 (0.0087)**	**0.68 (0.0023)**
Inlet Mouths	**0.92 (0.0000)**	-	**0.65 (0.0277)**	-
River Mouth	0.61 (0.0857)	**0.65 (0.0111)**	**0.70 (0.0076)**	**0.70 (0.0013)**

Tensile strength is a major source of uncertainty. While 5 kPa represents lower-bound values associated with early or late season ice, mid-winter strengths are typically higher (Figure 10; Johnston, 2017). Using more realistic strength values (e.g., ≥10 kPa) would require wind speeds well in excess of 100 km/h or current speeds >60 cm/s to generate the same fracture spacing. Taken together, these results indicate that wind and current forcing alone are insufficient to explain fracture initiation in Admiralty Inlet, implying that additional processes or pre-existing weaknesses play a primary role.

6.2.4 Promontory points and river mouths

There are more promontory points on the west shore (n=27; 21%) compared to the east shore (n=11; 9%), but several secondary inlets open along the eastern shore, which we categorize and count separately as inlet mouths (n=16; 12%). We identified 14 shoreline points associated with river mouths along the east shore (10%), and 25 river mouth shoreline points along the western shore (20%). There was no clear pattern in promontory point and river mouth point spacing along either shore, but inlet mouth points are generally spaced 5 km to 7.5 km apart along the eastern shore.

Given these shoreline point distributions, we evaluated whether fracture locations corresponded systematically to promontory points, river mouths, or inlet openings. Qualitatively, we observed indications of a relationship between the locations of fractures and promontory points and inlet mouths of different length categories (Figure 8). Quantitatively, we identified a strong ($p < 0.05$) connection between promontory points and both ends of fractures that extended fully across the inlet and short fractures that extended from the western shore (Table 4). River mouth points showed the same pattern with $p < 0.05$. Both short fractures and the eastern ends of long fractures showed strong relationships with the opening of inlets ($p < 0.05$), which occurred only along the eastern shore. There was no significant relationship ($p > 0.05$) between short fractures extending from the east shore and promontory points or river mouths.

7 Discussion

To interpret these results in a broader physical context, we now synthesize the spatial and temporal patterns of sea ice fractures in Admiralty Inlet described in Sections 6.1 with the environmental and geographical controls evaluated in Sections 6.2. We argue that seasonal variations in ice properties and environmental forcings primarily determine *when* fractures form (Sections 7.1 and 7.2). In contrast, spatial variations in ice material properties and locations of environmental stresses concentration

https://doi.org/10.5194/egusphere-2026-3739
Preprint. Discussion started: 2 July 2026

influence *where* fractures initiate, particularly fractures that form consistently in specific regions (Section 7.3). We further examine how ice properties and environmental forcings can influence subsequent fracture growth and widening (Sections 7.4 and 7.5). Although limitations in the fracture and environmental datasets prevent us from directly linking specific fractures to individual forcing events, the relative contributions of different processes across space and time provide insight into the conditions under which each factor becomes more or less important. Together, these insights identify priorities for future observational and modelling studies needed to improve understanding and prediction of landfast ice fracture (Section 7.6).

7.1 Seasonal patterns in fracture formation

Our results showed strong seasonal variability in fracture occurrence and in the environmental and material properties that influence fracture initiation. Although these factors also vary spatially, we address this variability in Section 7.3, while here we focus on their temporal evolution.

In the early winter (e.g., December and January), sea ice in Admiralty Inlet begins to form and consolidate, with lower strength, making it more susceptible to fracturing from external stresses such as wind/current stresses than later in the year when the ice is colder and thicker (Figure 10). If there is little wind, wave, or current action during freeze-up, and/or slow decreases in air temperature, the ice will grow more homogeneously, reducing the porosity of the ice, thus increasing its strength (Petrich and Eicken, 2017; Timco and Weeks, 2010). If the ice forms under more stormy conditions, greater wind, wave, and current action will lead to the formation of ice pans and pancakes that eventually consolidate into an inhomogeneous ice sheet. Rapid decreases in temperature can cause more porous ice to form. Differences in freeze-up conditions, in combination with other factors, likely contribute to why fractures form in similar, but not identical locations from year to year.

Fewer fractures were observed in April and May (Figure 9), which may be explained by both remote sensing detection limitations and physical processes. InSAR images begin to lose coherence in April and May, but fractures are generally too narrow to be observed in optical imagery during these months, lowering the number of fractures that can be identified (Loewen et al., 2026). While this may reduce the number of fractures we observe in these months, physical processes likely play a larger role. Air temperatures are still well below 0 °C from March to mid-May, which can cause ice to form in open fractures, thereby reducing the number of detectable features. In addition, the ice is thicker and snow is deeper at this time of year, requiring longer and more pronounced cold events to cause changes to upper ice surface temperatures. As a result, we expect weaker thermal stresses within the ice which would reduce fracture formation (Figure 11). Inuit Knowledge corroborates this seasonal pattern, emphasizing that fractures often undergo cycles of opening, refreezing, and reopening, particularly in relation to the lunar cycle, and tend to recur in approximately the same locations highlighted in several Inuit communities (Laidler and Ikummaq, 2008; Laidler et al., 2008; Laidler and Elee, 2008; Wilson et al., 2021).

In June and July, the ice thins and increases in porosity as brine channels expand, reducing ice strength (Figure 10, Timco and Weeks, 2010; Johnston, 2017; Frantz et al., 2019). While we do not expect thermal cracking to occur at this time of year due to reduced temperature fluctuations (Figure 11), and a reduced coefficient of thermal expansion (Kaidel et al., 2025), melting will occur preferentially along the shore as air temperatures and shortwave and longwave radiation increase and rivers begin to

https://doi.org/10.5194/egusphere-2026-3739
Preprint. Discussion started: 2 July 2026

thaw (Santella et al., 2021). Open water along the shoreline allows the landfast ice cover to become more susceptible to motion as a response to wind or currents, facilitating the (re)opening of fractures (Loewen et al., 2025).

7.2 Episodic events

Our estimates of environmental stresses suggest that sudden fracture due to wind or current stresses are unlikely except during extreme wind and/or current events (Figure 12). However, because König Beatty and Holland's (2010) analytical model does not account for fatigue or stress accumulation during multi-day events, episodic wind or current events may still weaken the ice over time or propagate existing fractures, even if they are insufficient to induce instantaneous tensile failure. Other *in-situ* studies of fracturing in sea ice have suggested that some fractures can open under low-stress conditions or due to fatigue failure (Kovalev et al., 2020; Parno et al., 2022; Langhorne et al., 2001).

Uncertainties in sea ice rheology and strength complicate efforts to link environmental events to fracture formation. Field measurements of how landfast ice strength evolves through the season are needed to better constrain this parameter. These uncertainties are compounded by the fact that ice deformation involves not only brittle failure but also creep, viscoelastic, and fatigue processes (Weiss and Dansereau, 2017). Our application of König Beatty and Holland's (2010) model does not account for these processes, and developing effective representations of fracture processes for landfast ice in sea ice models remains an active area of research (Bourgett et al., 2025; McKenna et al., 2021; Plante et al., 2020).

Due to the 12-day temporal resolution of InSAR data from Sentinel-1 and the variable temporal availability of usable Sentinel-2 data of approximately 1 to 7 days, it is difficult to attribute the formation of specific fractures to air temperatures, winds, or tides, since these factors fluctuate on daily to subdaily timescales. Instead, the Loewen et al. (2026) dataset is most useful for evaluating seasonal fracture patterns. Higher (subdaily) temporal resolution fracture location data are needed to directly connect episodic environmental events to fracture initiation. Community-based environmental monitoring efforts could fill this gap.

7.3 Spatial factors that lead to fracture formation

Persistent geographic constraints like coastal morphology and bathymetry create spatial variations in ice material properties and stress concentrations, which can be heightened during episodic environmental stress peaks, likely contribute to fracture initiation. We saw clear spatial patterns in fracture formation that recurred across years (Figure 4), which we attribute partially to the locations of promontory points, side inlets mouths, and river mouths (Table 4). Characteristics of promontory points and river mouths such as bathymetry gradients near the point, how far the point protrudes, and the magnitude of freshwater input into the ocean may impact these relationships, but investigating these variables is beyond the scope of this work.

Additional mechanisms may help explain the regular spacing pattern observed between fracture peaks (Figure 7). Inherent sea ice properties could influence how wind stress accumulates over specific regions of the ice cover (König Beatty and Holland, 2010). Flexural stresses might also concentrate at nodal points due to constructive interference of surface waves within Admiralty Inlet (Kovalev et al., 2020). The tendency for fractures to form perpendicular to the shoreline, with limited curvature (Table 2) suggests that the dominant stresses are oriented perpendicular to the shoreline. Numerical modelling of

https://doi.org/10.5194/egusphere-2026-3739
Preprint. Discussion started: 2 July 2026

these processes individually, and in combination, would help characterize the relative contributions and magnitude of these effects.

Wind speeds and directions in Admiralty Inlet are strongly influenced by mesoclimate effects driven by topography, similar to other locations in this part of the Canadian Arctic Archipelago (Moore and Imrit, 2022; Gearheard et al., 2010). Admiralty Inlet is bordered by steep cliffs on both sides (Figure 2), which result in pronounced topographic wind channelling. This creates kilometre-scale variations in wind speed, including areas of consistently stronger winds, which are well known to Ikpiarjukmiut. Localized wind patterns can generate spatially variable stress fields that may influence where fractures initiate.

Similarly, waves and ocean currents are influenced by bathymetry (Timmermans and Marshall, 2020). Although the central basin of Admiralty Inlet reaches substantial depths, many of the significant ice-ocean interactions occur in the comparatively shallow nearshore zone or at bathymetric constrictions such as sills or promontory points. These are locations where currents accelerate and wave heights increase. Other factors affecting ice bending stresses include wave-driven sea surface fluctuations and large-scale variations in sea surface height caused by tides or atmospheric pressure gradients, but these effects are not well-constrained for landfast ice (Langhorne et al., 2001; Quartly et al., 2019).

7.4 Fracture growth and refreezing

Based on our analysis of fracture growth characteristics (Table 3) and the relationship between fracture types and promontory points (Table 4), we hypothesize that short fractures are typically created by the lengthening of pre-existing flaws that form near the shoreline, while long fractures are more likely initiated by full-scale tensile or flexural failure mechanisms. This interpretation aligns with the conceptual model proposed by Lewis (1995), in which initial flaws (e.g., surface cracks that do not penetrate the full ice thickness) first propagate horizontally before extending vertically, eventually splitting the ice. Shallow surface cracks are also common in Admiralty Inlet, named *nuttaq* by Ikpiarjukmiut (Tuvaliriji Committee et al., 2025), suggesting that similar fracture initiation processes occur locally.

We build on this conceptual model by proposing that many fractures initially form when the ice is thin and the stresses required to exceed ice strength are relatively low. These initiating stresses may result from thermal gradients, enhanced current forces, such as those associated with spring tides, and/or short-duration atmospheric events. Once formed, these fractures may be sustained or extended by recurring external stresses, including tidal cycles and wind forcing. Since a fracture already exists, either partially or fully though the thickness of the ice, these stresses do not need to be very high to maintain or lengthen the fracture at the crack tip (Dempsey et al., 2018; Lewis, 1995). Spatial variations in ice mechanical properties may predispose certain regions of the ice cover to fracture more readily under external stress. Once the initial fractures form, only those located near stress concentrations (e.g., promontory points) are more likely to persist and evolve.

This conceptual model may help explain the initiation of both short and long fractures, the key difference being the spatial scale of the initial flaw in the ice, and/or the time required for it to propagate horizontally and vertically through the ice. The 12-day repeat interval of Sentinel-1 InSAR may be insufficient to capture the gradual formation of fractures in the winter that span the inlet, which may explain why they appear to form suddenly. In contrast, localized stress concentrations may lead to short fractures that do not extend across the inlet, as these stresses are relieved over a more confined area. Most short fractures

https://doi.org/10.5194/egusphere-2026-3739
Preprint. Discussion started: 2 July 2026

appear to grow away from the shore, as opposed to forming in the middle of the inlet and growing towards shore(s) (Table 3). This pattern aligns with the presence of stress concentrations at the shoreline driven by bathymetric and topographic changes, and variations in the shoreline direction (e.g., promontory points).

Seasonal patterns in fracture formation also align with this model. Many fractures open in early winter when ice is relatively weak, while fewer form in mid-winter when ice strength peaks (Figures 10, 9). In late spring, although the ice is thicker, rising air and ice temperatures reduce ice strength, making it more susceptible to fracturing. Our observations suggest that localized nearshore stress concentrations may persist year-round, enabling fracture reactivation in spring. Ikpiarjukmiut have observed that some *aajurait* open in the same places as winter *nagguti*, though they sometimes follow different paths across the ice, resulting in new fracture locations. Similar reactivation and redirection of ice fractures have been observed in laboratory experiments (Murdza et al., 2022) and *in-situ* observations (Fedders, 2025), and we observe this pattern in our fracture dataset as well. Offshore, seasonal shifts in stress concentrations may reflect evolving gradients in ice properties as the ice thickens, or changes in environmental forcing.

As air and ocean temperatures in the Arctic increase, thermal influences on ice fracturing and refreezing may be altered, affecting when and where fractures form. Further observational and numerical modelling studies are needed to explore these seasonal and process-level dynamics in greater detail.

7.5 Fracture widening

The processes that lead to fracture opening and widening are similar, but mechanically, much less stress at the 'crack tip' is required to widen a fracture that has already opened, provided there is a way for the ice to separate. A fracture may widen due to thermodynamic melting of ice along the edges of the fracture, mechanical erosion along the fracture edges, and/or divergence of ice on either side of the fracture (Figure 13).

The width of a fracture affects its mechanical role. Narrow fractures may not significantly affect stress distributions within an ice sheet, but eventually, a fracture may become wide enough to enable ice motion and influence subsequent fracture formation (Fedders, 2025). Knowing fracture width is also important for safe travel on sea ice, and developing methods to estimate metre-scale fracture widths from satellite imagery would be beneficial to sea ice users.

While these widening processes are important for both ice mechanics and navigation, detecting and quantifying them using satellite imagery remains challenging. Due to limitations in our methods, we cannot measure how wide a fracture is open or if it widens (or narrows) over time. It is also challenging to determine whether a fracture that appears to extend only partway across the inlet truly does so, or whether its full extent cannot be captured in satellite imagery. We can observe fractures that are wide enough to be seen in satellite imagery, but this only gives us a lower bound on the fracture width, not a definitive measurement. Consequently, the processes governing fracture widening remain poorly constrained at spatial and temporal scales relevant to both ice dynamics and community use. Addressing these gaps will require new approaches for detecting narrow fractures, tracking their evolution, and integrating observations with modelling frameworks.

https://doi.org/10.5194/egusphere-2026-3739
Preprint. Discussion started: 2 July 2026

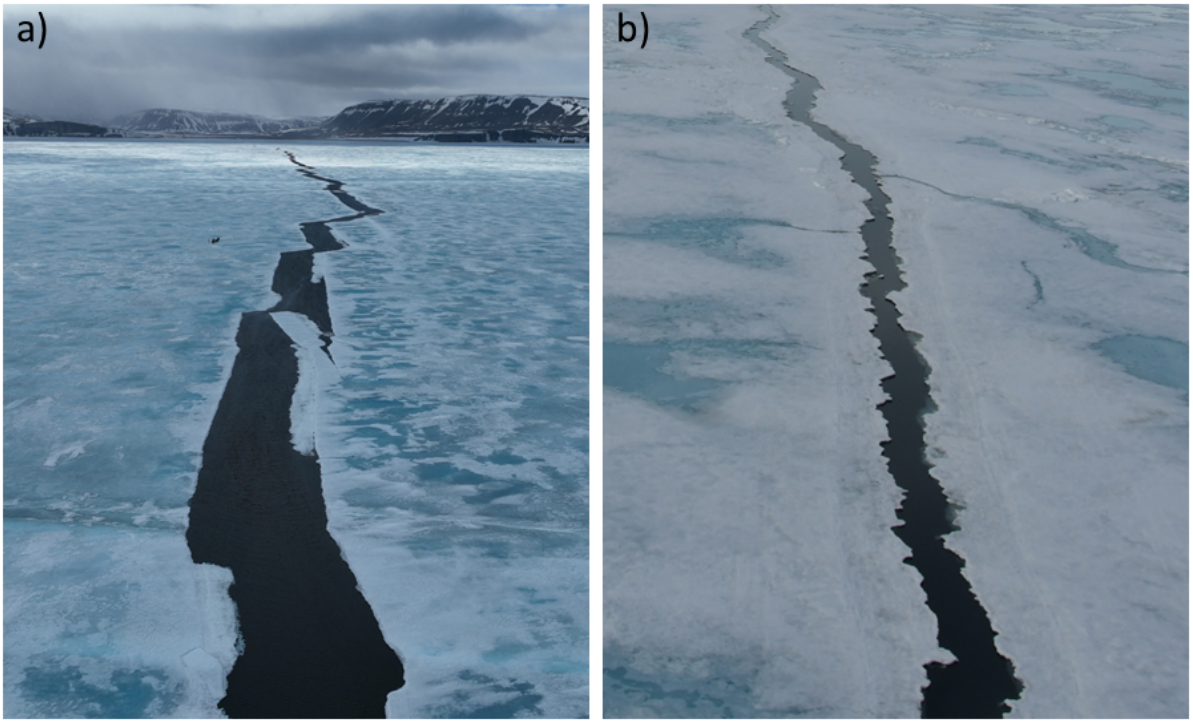

Figure 13. Aerial photos of fracture widening by gradual breaking off of pieces along the fracture edges (a) and melting of ice along the edges of the fracture (b). Note the jagged edges along the fracture in (b) which indicate that this fracture recently opened.

7.6 Recommendations

In this paper, we identified key processes that lead to fracture in confined landfast sea ice. However, substantial gaps remain in environmental observations and in understanding how different forcings interact, which limits our ability to link specific conditions to the formation of individual fractures. To advance the study of fracture processes, we outline several observational and modelling needs.

Key observational gaps include:

- Daily or sub-daily remote sensing and time-lapse imagery of ice conditions,
- Nearshore sea surface height/sea-level pressure,
- Ocean current measurements under landfast sea ice,
- Metre-scale nearshore bathymetry,
- Weather stations in areas influenced by topographic effects, and
- Seasonal geophysical-scale ice strength measurements.

https://doi.org/10.5194/egusphere-2026-3739
Preprint. Discussion started: 2 July 2026

Improving numerical representations of landfast sea ice will require advances in both physical parameterizations and process-level experimentation. We recommend that future modelling studies:

- Develop dynamic ice grounding schemes that vary with tides and seasons for landfast ice,
- Compare viscous-plastic and brittle rheologies to recreate observed fracture patterns in landfast sea ice, and
- Individually evaluate the contributions of wind, tides, thermal gradients, and currents to fracture formation.

We also highlight the mutual benefits of working with the local community throughout this research process, whose knowledge provided important context for interpreting how local geographical and environmental factors influence fracture dynamics in Admiralty Inlet. While we recognize that that research programs differ in capacity for direct collaboration, we suggest academic scientists review existing Inuit Knowledge descriptions of local ice and environmental conditions, where such materials are publicly shared, and, where possible, engage early with relevant community organizations to identify shared priorities, travel safety concerns, and opportunities for knowledge exchange. Numerous resources exist to support researchers in developing reciprocal, respectful research relationships (e.g., ITK and NRI, 2007; Inuit Circumpolar Council, 2021; Wilson et al., 2020; Bishop et al., 2025).

Although significant uncertainties remain that limit accurate predictions of when and where fractures will form, the results of this study affirm existing Inuit Knowledge of sea ice behaviour and highlight several locally observable conditions that may increase fracture susceptibility. Examples include thin ice, existing open fractures, spring tides, and strong winds, which may act together to trigger the formation of new fractures. Community-based environmental monitoring programs such as the Sikumik Qaujimajjuti ('tools to know how the ice is') program (Beaulieu et al., 2023), SIKU (www.siku.org) and Silanga (silanga.ca) can complement Inuit Knowledge by supporting real-time ice assessments and generating locally relevant environmental datasets. These programs strengthen safety planning while generating high-resolution observations needed to address many of the outstanding research questions identified in this study that can support community needs.

8 Conclusions

In this paper, we examined the spatial and temporal patterns of fractures in seasonal landfast ice in Admiralty Inlet, Nunavut, a deep water fiord. Similar patterns are likely to occur in other confined waterways in polar regions such as the Canadian Arctic Archipelago. Consistent seasonal changes in ice strength and environmental stresses drove temporal patterns in fracturing events, while we surmise that geographic factors concentrated stresses in certain locations (e.g., promontory points), driving recurring patterns in fracture formation. Interannual variability in environmental driving forces and sea ice properties likely drove variability in these patterns.

Fractures generally initiated at the shoreline, propagated perpendicular to the shore, and subsequently lengthened toward the middle or the other end of the inlet, with little curvature. Fracture length is thought to reflect the magnitude and distribution of local stress concentrations, but further work is needed to quantify this effect. We were unable to associate specific fracturing

https://doi.org/10.5194/egusphere-2026-3739
Preprint. Discussion started: 2 July 2026

events with the associated environmental stresses due to the limited availability of satellite data to observe fractures and environmental data within Admiralty Inlet. However, we expect episodic events to influence some fracturing events.

While ongoing changes in the Arctic climate are expected to reshape the conditions under which fractures form, the results of this study summarize the current understanding of fractures in confined landfast ice and identify priorities for further observations and modelling to answer outstanding questions.

Data availability. The satellite-derived fracture dataset is available at www.polardata.ca/pdcsearch/PDCSearchDOI.jsp?doi_id=13410. Shoreline geometry data were modified from https://open.canada.ca/data/en/dataset/a883eb14-0c0e-45c4-b8c4-b54c4a819edb (last access 24 June 20 26). Version 4.0 of the International Bathymetric Chart of the Arctic Ocean (IBCAO; Jakobsson et al. (2020)) was acquired from https://gebco.net (last access 24 June 2026), and ERA5 data (Hersbach et al., 2025) were downloaded from the Copernicus Climate Data Store (https://cds.climate.copernicus.eu/, last access 24 June 2026). The Webtide Tidal Prediction Model application can be downloaded from https://www.bio.gc.ca/science/research-recherche/ocean/webtide/index-en.php (last access 24 June 2026). The SmartQAMUTIK and Inuit Knowledge datasets presented in this article require permission from the Tuvaliriji Committee for access. Requests to access the SmartQAMUTIK and Inuit Knowledge datasets should be directed to Katherine Wilson, katherine@smartice.org.

Author contributions. AL, DM, GC, and AM participated in the conceptualization of the research plan. AL, KW, and AMQ conducted Inuit Knowledge workshops in Ikpiarjuk, NU. AL carried out the analysis and prepared the manuscript. All authors reviewed and edited the manuscript.

Competing interests. The authors declare that they have no conflict of interest.

Acknowledgements. We thank Arctic Bay Adventures for their field support and the Polar Continental Shelf Program for helicopter support. We also thank the late Mishak Allurut, the Ikajutit HTA, and the Tuvaliriji SmartICE community management committee in Ikpiarjuk for sharing their knowledge over many enriching conversations about sea ice.

Financial support. This research was supported by the Crown-Indigenous Relations and Northern Affairs Canada Climate Change Preparedness in the North Program project 'Landfast Sea Ice Breakup Prediction in a Changing Climate,' an Environment and Climate Change Canada grant, and the ArcticNet (a Network of Centers of Excellence of Canada) Project 'Weather and aajurait (lead) Monitoring for sea ice safety during the break-up season' which was endorsed as a UN Ocean Decade Action and run in partnership with SmartICE and the Canadian Ice Service. Ada Loewen was financially supported by the Northern Research Training Program, the Ontario Graduate Scholarship, the National Sciences and Engineering Research Council of Canada, and Carleton University scholarships.

https://doi.org/10.5194/egusphere-2026-3739
Preprint. Discussion started: 2 July 2026

References

Archer, L., Ford, J. D., Pearce, T., Kowal, S., Gough, W. A., and Allurut, M.: Longitudinal assessment of climate vulnerability: a case study from the Canadian Arctic, Sustainability Science, 12, 15–29, https://doi.org/10.1007/s11625-016-0401-5, publisher: Springer Tokyo, 2017.

Beaulieu, L., Arreak, A., Holwell, R., Dicker, S., Qamanirq, O., Moorman, L., Wilson, K., Segal, R., Crichton, S., and Bell, T.: Indigenous self-determination in cryospheric science: The Inuit-led Sikumik Qaujimajjuti ("tools to know how the ice is") program in Inuit Nunangat, Canada, Frontiers in Earth Science, 11, 2023.

Bell, T., Arreak, A., and Mosesie, J.: Inuit Qaujimajatuqangit of Landfast Ice Breakup in Admiralty Inlet, Tech. Rep. 19-11, SmartICE, Arctic Bay, NU, 2019.

Bigdeli, A., Nguyen, A. T., Pillar, H. R., Ocaña, V., and Heimbach, P.: Atmospheric Warming Drives Growth in Arctic Sea Ice: A Key Role for Snow, Geophysical Research Letters, 47, e2020GL090 236, https://doi.org/https://doi.org/10.1029/2020GL090236, 2020.

Bishop, B., Denniston, M., Oliver, E. C., and Aporta, C.: An Iterative and Participatory Method for Mapping Inuit Knowledge of the Ice and Ocean in Nunatsiavut, Human Ecology, https://doi.org/10.1007/s10745-025-00631-8, 2025.

Bouchat, A., Hutter, N., Chanut, J., Dupont, F., Dukhovskoy, D., Garric, G., Lee, Y. J., Lemieux, J.-F., Lique, C., Losch, M., Maslowski, W., Myers, P. G., Ólason, E., Rampal, P., Rasmussen, T., Talandier, C., Tremblay, B., and Wang, Q.: Sea Ice Rheology Experiment (SIREx): 1. Scaling and Statistical Properties of Sea-Ice Deformation Fields, Journal of Geophysical Research: Oceans, 127, e2021JC017 667, https://doi.org/10.1029/2021JC017667, 2022.

Bourgett, M., Losch, M., and Plante, M.: Comparing heterogeneity of sea-ice models with viscous-plastic and Maxwell elasto-brittle rheology, Annals of Glaciology, 66, e4, https://doi.org/10.1017/aog.2024.40, 2025.

Canadian Ice Service: Canadian Ice Thickness Program Ice thickness data, https://www.canada.ca/en/environment-climate-change/services/ice-forecasts-observations/latest-conditions/archive-overview/thickness-data.html, last Modified: 2024-07-18, 2024.

Collins, A. K., Hannah, C. G., and Greenberg, D.: Validation of a High Resolution Modelling System for Tides in the Canadian Arctic Archipelago, Can. Tech. Rep. Hydrogr. Ocean Sci. 273, Canadian Hydrographic Service, 2011.

Dempsey, J. P., Cole, D. M., and Wang, S.: Tensile fracture of a single crack in first-year sea ice, Philosophical Transactions of the Royal Society A: Mathematical, Physical and Engineering Sciences, 376, 20170 346, https://doi.org/10.1098/rsta.2017.0346, 2018.

Denis, D. J.: Analysis of Variance, in: Applied Univariate, Bivariate, and Multivariate Statistics Using Python: A Beginner's Guide to Advanced Data Analysis, John Wiley & Sons, Incorporated, Newark, UNITED STATES, ISBN 978-1-119-57817-8, 2021.

Environment and Climate Change Canada: Nanisivik Canadian Climate Normals 1981-2010, https://climate.weather.gc.ca/climate_normals/results_1981_2010_e.html?searchType=stnProv&lstProvince=NU&txtCentralLatMin=0&txtCentralLatSec=0&txtCentralLongMin=0&txtCentralLongSec=0&climate_id=2402730&dispBack=0, 2026.

E.U. Copernicus Marine Service Information (CMEMS). Marine Data Store (MDS).: Global Ocean Physics Analysis and Forecast, https://doi.org/10.48670/moi-00016, 2024.

Evans, R. J. and Untersteiner, N.: Thermal cracks in floating ice sheets, Journal of Geophysical Research (1896-1977), 76, 694–703, https://doi.org/10.1029/JC076i003p00694, 1971.

Fedders, E. R.: Sea ice strain, stress, and fracture activity at kilometer scales, Ph.D. thesis, University of Alaska Fairbanks, 2025.

https://doi.org/10.5194/egusphere-2026-3739
Preprint. Discussion started: 2 July 2026

Fedders, E. R., Mahoney, A. R., Dammann, D. O., Polashenski, C., and Hutchings, J. K.: Two-dimensional thermal and dynamical strain in landfast sea ice from InSAR: results from a new analytical inverse method and field observations, Annals of Glaciology, pp. 1–14, https://doi.org/10.1017/aog.2024.29, 2024.

Fedders, E. R., Mahoney, A. R., Polashenski, C., Hutchings, J. K., and Richter-Menge, J. A.: Effective Elastic Parameters for In Situ, Drifting Sea Ice Under Natural Forcing Conditions at Kilometer Scales, Journal of Geophysical Research: Oceans, 130, e2025JC022 400, https://doi.org/10.1029/2025JC022400, 2025.

Fissel, D. B. and Wilton, G. R.: Subsurface Current Measurements in Eastern Lancaster Sound, NWT - Summer 1977, Tech. rep., Arctic Sciences Ltd., Sidney, B.C., 1978.

Ford, J. D., Clark, D., Pearce, T., Berrang-Ford, L., Copland, L., Dawson, J., New, M., and Harper, S. L.: Changing access to ice, land and water in Arctic communities, Nature Climate Change, 9, 335–339, https://doi.org/10.1038/s41558-019-0435-7, iSBN: 4155801904357, 2019.

Fox, C. and Squire, V. A.: On the Oblique Reflexion and Transmission of Ocean Waves at Shore Fast Sea Ice, Philosophical Transactions: Physical Sciences and Engineering, 347, 185–218, 1994.

Fox, S., Crawford, A., McCrystall, M., Stroeve, J., Lukovich, J., Loeb, N., Natanine, J., and Serreze, M.: Extreme Arctic Weather and Community Impacts in Nunavut: A Case Study of One Winter's Storms and Lessons for Local Climate Change Preparedness, Weather, Climate, and Society, 15, 881–892, https://doi.org/10.1175/WCAS-D-23-0006.1, 2023.

Frantz, C. M., Light, B., Farley, S. M., Carpenter, S., Lieblappen, R., Courville, Z., Orellana, M. V., and Junge, K.: Physical and optical characteristics of heavily melted "rotten" Arctic sea ice, The Cryosphere, 13, 775–793, https://doi.org/10.5194/tc-13-775-2019, 2019.

Gearheard, S., Pocernich, M., Stewart, R., Sanguya, J., and Huntington, H. P.: Linking Inuit knowledge and meteorological station observations to understand changing wind patterns at Clyde River, Nunavut, Climatic Change, 100, 267–294, https://doi.org/10.1007/s10584-009-9587-1, 2010.

Hata, Y. and Tremblay, L. B.: Anisotropic internal thermal stress in sea ice from the Canadian Arctic Archipelago, Journal of Geophysical Research: Oceans, 120, 5457–5472, https://doi.org/https://doi.org/10.1002/2015JC010819, 2015.

Hersbach, H., Bell, B., Berrisford, P., Biavati, G., Horányi, A., Muñoz Sabater, J., Nicolas, J., Peubey, C., Radu, R., Rozum, I., Schepers, D., Simmons, A., Soci, C., Dee, D., and Thépaut, J.-N.: ERA5 hourly data on single levels from 1979 to present., https://doi.org/10.24381/cds.adbb2d47, 2025.

Heyes, S. A.: Cracks in the knowledge: sea ice terms in Kangiqsualujjuaq, Nunavik, The Canadian Geographer / Le Géographe canadien, 55, 69–90, https://doi.org/10.1111/j.1541-0064.2010.00346.x, publisher: John Wiley & Sons, Ltd (10.1111), 2011.

Hoffman, J. P., Ackerman, S. A., Liu, Y., and Key, J. R.: A 20-Year Climatology of Sea Ice Leads Detected in Infrared Satellite Imagery Using a Convolutional Neural Network, Remote Sensing, 14, 5763, https://doi.org/10.3390/rs14225763, 2022.

Hui, F., Li, X., Zhao, T., Shokr, M., Heil, P., Zhao, J., Liu, Y., Liang, S., and Cheng, X.: Semi-Automatic Mapping of Tidal Cracks in the Fast Ice Region near Zhongshan Station in East Antarctica Using Landsat-8 OLI Imagery, Remote Sensing, 8, 242, https://doi.org/10.3390/rs8030242, 2016.

Hunke, E. C., Allard, R., Blain, P., Blockley, E., Feltham, D., Fichefet, T., Garric, G., Grumbine, R., Lemieux, J. F., Rasmussen, T., Ribergaard, M., Roberts, A., Schweiger, A., Tietsche, S., Tremblay, B., Vancoppenolle, M., and Zhang, J.: Should Sea-Ice Modeling Tools Designed for Climate Research Be Used for Short-Term Forecasting?, Current Climate Change Reports, 6, 1–16, https://doi.org/10.1007/s40641-020-00162-y, 2020.

https://doi.org/10.5194/egusphere-2026-3739
Preprint. Discussion started: 2 July 2026

Hutter, N., Bouchat, A., Dupont, F., Dukhovskoy, D., Koldunov, N., Lee, Y. J., Lemieux, J.-F., Lique, C., Losch, M., Maslowski, W., Myers, P. G., Ólason, E., Rampal, P., Rasmussen, T., Talandier, C., Tremblay, B., and Wang, Q.: Sea Ice Rheology Experiment (SIREx): 2. Evaluating Linear Kinematic Features in High-Resolution Sea Ice Simulations, Journal of Geophysical Research: Oceans, 127, e2021JC017 666, https://doi.org/10.1029/2021JC017666, 2022.

Inuit Circumpolar Council: Ethical and Equitable Engagement Synthesis Report: A collection of Inuit rules, guidelines, protocols, and values for the engagement of Inuit Communities and Indigenous Knowledge from Across Inuit Nunaat, Tech. rep., Inuit Circumpolar Council, https://iccalaska.org/wp-icc/wp-content/uploads/2021/09/ICC-EEE-Synthesis-report.pdf, 2021.

ITK and NRI: Negotiating Research Relationships with Inuit Communities: A Guide for Researchers, Tech. rep., Inuit Tapiriit Kanatami and Nunavut Research Institute, Ottawa and Iqaluit, 2007.

Jakobsson, M., Mayer, L. A., Bringensparr, C., Castro, C. F., Mohammad, R., Johnson, P., Ketter, T., Accettella, D., Amblas, D., An, L., Arndt, J. E., Canals, M., Casamor, J. L., Chauché, N., Coakley, B., Danielson, S., Demarte, M., Dickson, M.-L., Dorschel, B., Dowdeswell, J. A., Dreutter, S., Fremand, A. C., Gallant, D., Hall, J. K., Hehemann, L., Hodnesdal, H., Hong, J., Ivaldi, R., Kane, E., Klaucke, I., Krawczyk, D. W., Kristoffersen, Y., Kuipers, B. R., Millan, R., Masetti, G., Morlighem, M., Noormets, R., Prescott, M. M., Rebesco, M., Rignot, E., Semiletov, I., Tate, A. J., Travaglini, P., Velicogna, I., Weatherall, P., Weinrebe, W., Willis, J. K., Wood, M., Zarayskaya, Y., Zhang, T., Zimmermann, M., and Zinglersen, K. B.: The International Bathymetric Chart of the Arctic Ocean Version 4.0, Scientific Data, 7, 176, https://doi.org/10.1038/s41597-020-0520-9, publisher: Nature Publishing Group, 2020.

Jewell, M. E., Hutchings, J. K., and Geiger, C. A.: Atmospheric highs drive asymmetric sea ice drift during lead opening from Point Barrow, The Cryosphere, 17, 3229–3250, https://doi.org/10.5194/tc-17-3229-2023, publisher: Copernicus GmbH, 2023.

Johnston, M. E.: A comparison of physical properties and strength of decaying first-year ice in the Arctic and sub-Arctic, Annals of Glaciology, 44, 154–162, 2006.

Johnston, M. E.: Seasonal changes in the properties of first-year, second-year and multi-year ice, Cold Regions Science and Technology, 141, 36–53, https://doi.org/10.1016/j.coldregions.2017.05.006, 2017.

Jones, J., Eicken, H., Mahoney, A., MV, R., Kambhamettu, C., Fukamachi, Y., Ohshima, K. I., and George, J. C.: Landfast sea ice breakouts: Stabilizing ice features, oceanic and atmospheric forcing at Barrow, Alaska, Continental Shelf Research, 126, 50–63, https://doi.org/10.1016/j.csr.2016.07.015, 2016.

Kaidel, L., Polashenski, C., Wright, N., Fedders, E. R., and Mahoney, A. R.: In Situ Observations of the Thermal Strain Coefficient of Sea Ice, Geophysical Research Letters, 52, e2024GL111 434, https://doi.org/10.1029/2024GL111434, 2025.

Kerby, D. S.: The Simple Difference Formula: An Approach to Teaching Nonparametric Correlation1, Comprehensive Psychology, 3, 11.IT.3.1, https://doi.org/10.2466/11.IT.3.1, 2014.

Kovalev, D. P., Kovalev, P. D., and Squire, V. A.: Crack formation and breakout of shore fast sea ice in Mordvinova Bay, south-east Sakhalin Island, Cold Regions Science and Technology, 175, 103 082, https://doi.org/https://doi.org/10.1016/j.coldregions.2020.103082, 2020.

Kowal, S., Gough, W. A., and Butler, K.: Temporal and Spatial Evolution of Seasonal Sea Ice of Arctic Bay, Nunavut, Coasts, 3, 113–124, https://doi.org/10.3390/coasts3020007, 2023.

Krupnik, I.: 'How many Eskimo words for ice?' Collecting Inuit sea ice terminologies in the International Polar Year 2007–2008, Canadian Geographer / Le Géographe canadien, 55, 56–68, https://doi.org/10.1111/j.1541-0064.2010.00345.x, 2011.

König Beatty, C. and Holland, D. M.: Modeling Landfast Sea Ice by Adding Tensile Strength, Journal of Physical Oceanography, 40, 185–198, https://doi.org/10.1175/2009JPO4105.1, 2010.

https://doi.org/10.5194/egusphere-2026-3739
Preprint. Discussion started: 2 July 2026

Laidler, G. J.: Inuit and scientific perspectives on the relationship between sea ice and climate change: The ideal complement?, Climatic Change, 78, 407–444, https://doi.org/10.1007/s10584-006-9064-z, arXiv: 1011.1669v3 ISBN: 0165-0009, 2006.

Laidler, G. J. and Elee, P.: Human geographies of sea ice: freeze/thaw processes around Cape Dorset, Nunavut, Canada, Polar Record, 44, 51–76, https://doi.org/10.1017/S0032247407007061, 2008.

Laidler, G. J. and Ikummaq, T.: Human geographies of sea ice: freeze/thaw processes around Igloolik, Nunavut, Canada, Polar Record, 44, 127–153, https://doi.org/10.1017/S0032247407007152, 2008.

Laidler, G. J., Dialla, A., and Joamie, E.: Human geographies of sea ice: freeze/thaw processes around Pangnirtung, Nunavut, Canada, Polar Record, 44, 335–361, https://doi.org/10.1017/S003224740800750X, 2008.

Laidler, G. J., Ford, J. D., Gough, W. A., Ikummaq, T., Gagnon, A. S., Kowal, S., Qrunnut, K., and Irngaut, C.: Travelling and hunting in a changing Arctic: assessing Inuit vulnerability to sea ice change in Igloolik, Nunavut, Climatic Change, 94, 363–397, https://doi.org/10.1007/s10584-008-9512-z, 2009.

Laidler, G. J., Elee, P., Ikummaq, T., Joamie, E., and Aporta, C.: Mapping Inuit Sea Ice Knowledge, Use, and Change in Nunavut, Canada (Cape Dorset, Igloolik, Pangnirtung), in: SIKU: Knowing Our Ice, edited by Krupnik, I., Aporta, C., Gearheard, S., Laidler, G. J., and Kielsen Holm, L., pp. 45–80, Springer Netherlands, Dordrecht, https://doi.org/10.1007/978-90-481-8587-0_3, 2010.

Langhorne, P. J., Squire, V. A., Fox, C., and Haskell, T. G.: Lifetime estimation for a land-fast ice sheet subjected to ocean swell, Annals of Glaciology, 33, 333–338, https://doi.org/10.3189/172756401781818419, 2001.

Lemieux, J., Lei, J., Dupont, F., Roy, F., Losch, M., Lique, C., and Laliberté, F.: The Impact of Tides on Simulated Landfast Ice in a Pan-Arctic Ice-Ocean Model, Journal of Geophysical Research: Oceans, 123, 2018JC014 080, https://doi.org/10.1029/2018JC014080, 2018.

Lemieux, J.-F., Dupont, F., Blain, P., Roy, F., Smith, G. C., and Flato, G. M.: Improving the simulation of landfast ice by combining tensile strength and a parameterization for grounded ridges, Journal of Geophysical Research: Oceans, 121, 7354–7368, https://doi.org/10.1002/2016JC012006, 2016.

Lewis, J. K.: A conceptual model of the impact of flaws on the stress state of sea ice, Journal of Geophysical Research: Oceans, 100, 8829–8835, https://doi.org/10.1029/95JC00686, 1995.

Lewis, J. K., Tucker III, W. B., and Stein, P. J.: Observations and modeling of thermally induced stresses in first-year sea ice, Journal of Geophysical Research: Oceans, 99, 16 361–16 371, https://doi.org/10.1029/94JC01242, 1994.

Li, Z., Zhao, J., Su, J., Li, C., Cheng, B., Hui, F., Yang, Q., and Shi, L.: Spatial and temporal variations in the extent and thickness of arctic landfast ice, Remote Sensing, 12, 64, https://doi.org/10.3390/RS12010064, 2020.

Liu, Y., Losch, M., Hutter, N., and Mu, L.: A New Parameterization of Coastal Drag to Simulate Landfast Ice in Deep Marginal Seas in the Arctic, Journal of Geophysical Research: Oceans, 127, e2022JC018 413, https://doi.org/10.1029/2022JC018413, 2022.

Loewen, A., Crocker, G., Mueller, D., and McKenna, R.: The role of preconditioning on landfast sea ice break-off processes in Admiralty Inlet, Nunavut, Arctic Science, 11, 1–21, https://doi.org/10.1139/as-2024-0053, 2025.

Loewen, A., Crocker, G., Mueller, D., Wilson, K., and Mike-Qaunaq, A.: Connecting remote sensing, Inuit Knowledge, and *in-situ* observations for monitoring landfast sea ice fracture development in Admiralty Inlet, Nunavut, Canadian Journal of Remote Sensing, 52, 2614 141, https://doi.org/10.1080/07038992.2026.2614141, 2026.

Lu, P., Li, Z., Cheng, B., and Leppäranta, M.: A parameterization of the ice-ocean drag coefficient, Journal of Geophysical Research: Oceans, 116, https://doi.org/10.1029/2010JC006878, 2011.

https://doi.org/10.5194/egusphere-2026-3739
Preprint. Discussion started: 2 July 2026

Mahoney, A. R., Eicken, H., Gaylord, A. G., and Shapiro, L.: Alaska landfast sea ice: Links with bathymetry and atmospheric circulation, Journal of Geophysical Research, 112, C02 001, https://doi.org/10.1029/2006JC003559, publisher: John Wiley & Sons, Ltd ISBN: 0148-0227, 2007.

Mahoney, A. R., Dammann, D. O., Johnson, M., Eicken, H., and Meyer, F. J.: Measurement and imaging of infragravity waves in sea ice using InSAR, Geophysical Research Letters, 43, 6383–6392, https://doi.org/10.1002/2016GL069583, publisher: Blackwell Publishing Ltd, 2016.

Marcq, S. and Weiss, J.: Influence of sea ice lead-width distribution on turbulent heat transfer between the ocean and the atmosphere, The Cryosphere, 6, 143–156, https://doi.org/10.5194/tc-6-143-2012, 2012.

Maus, S.: The tensile strength of sea ice: revising its dependence on microstructure and growth velocity, in: Proceedings of the 27th International Conference on Port and Ocean Engineering under Arctic Conditions, Glasgow, United Kingdom, 2023.

Mchedlishvili, A., Lüpkes, C., Petty, A., Tsamados, M., and Spreen, G.: New estimates of pan-Arctic sea ice–atmosphere neutral drag coefficients from ICESat-2 elevation data, The Cryosphere, 17, 4103–4131, https://doi.org/10.5194/tc-17-4103-2023, 2023.

McKenna, R., Loewen, A., and Crocker, G.: A finite element model for the deformation of floating ice covers, Cold Regions Science and Technology, 182, 103 213, https://doi.org/10.1016/j.coldregions.2020.103213, 2021.

Moore, G. W. K. and Imrit, A. A.: Impact of Resolution on the Representation of the Mean and Extreme Winds Along Nares Strait, Journal of Geophysical Research: Atmospheres, 127, e2022JD037 443, https://doi.org/10.1029/2022JD037443, 2022.

Murdza, A., Schulson, E. M., Renshaw, C. E., and Polojärvi, A.: Rapid Healing of Thermal Cracks in Ice, Geophysical Research Letters, 49, e2022GL099 771, https://doi.org/10.1029/2022GL099771, _eprint: https://agupubs.onlinelibrary.wiley.com/doi/pdf/10.1029/2022GL099771, 2022.

Parno, J., Polashenski, C., Parno, M., Nelsen, P., Mahoney, A., and Song, A.: Observations of Stress-Strain in Drifting Sea Ice at Floe Scale, Journal of Geophysical Research: Oceans, 127, e2021JC017 761, https://doi.org/10.1029/2021JC017761, 2022.

Petrich, C. and Eicken, H.: Overview of sea ice growth and properties, in: Sea Ice, pp. 1–41, John Wiley & Sons, Ltd, ISBN 978-1-118-77837-1, https://doi.org/10.1002/9781118778371.ch1, 2017.

Petrich, C., Langhorne, P. J., and Haskell, T. G.: Formation and structure of refrozen cracks in land-fast first-year sea ice, Journal of Geophysical Research, 112, C04 006, https://doi.org/10.1029/2006JC003466, 2007.

Petty, A. A., Tsamados, M. C., and Kurtz, N. T.: Atmospheric form drag coefficients over Arctic sea ice using remotely sensed ice topography data, spring 2009-2015, Journal of Geophysical Research: Earth Surface, 122, 1472–1490, https://doi.org/10.1002/2017JF004209, 2017.

Plante, M., Tremblay, B., Losch, M., and Lemieux, J.-F.: Landfast sea ice material properties derived from ice bridge simulations using the Maxwell elasto-brittle rheology, The Cryosphere, 14, 2137–2157, https://doi.org/10.5194/tc-14-2137-2020, 2020.

Qikiqtani Inuit Association: Qikiqtani Truth Commission: Community Histories 1950-1975 - Arctic Bay, Tech. rep., Qikiqtani Inuit Association, Iqaluit, Nunavut, 2013.

Qu, M., Pang, X., Zhao, X., Lei, R., Ji, Q., Liu, Y., and Chen, Y.: Spring leads in the Beaufort Sea and its interannual trend using Terra/MODIS thermal imagery, Remote Sensing of Environment, 256, 112 342, https://doi.org/10.1016/j.rse.2021.112342, 2021.

Quartly, G. D., Rinne, E., Passaro, M., Andersen, O. B., Dinardo, S., Fleury, S., Guillot, A., Hendricks, S., Kurekin, A. A., Müller, F. L., Ricker, R., Skourup, H., and Tsamados, M.: Retrieving Sea Level and Freeboard in the Arctic: A Review of Current Radar Altimetry Methodologies and Future Perspectives, Remote Sensing, 11, 881, https://doi.org/10.3390/rs11070881, 2019.

Reiser, F., Willmes, S., Hausmann, U., and Heinemann, G.: Predominant Sea Ice Fracture Zones Around Antarctica and Their Relation to Bathymetric Features, Geophysical Research Letters, 46, 12 117–12 124, https://doi.org/10.1029/2019GL084624, 2019.

https://doi.org/10.5194/egusphere-2026-3739
Preprint. Discussion started: 2 July 2026

Richter-Menge, J. A. and Elder, B. C.: Characteristics of pack ice stress in the Alaskan Beaufort Sea, Journal of Geophysical Research: Oceans, 103, 21 817–21 829, https://doi.org/10.1029/98JC01261, 1998.

Santella, G. E., Gallaher, S. G., and Smith, J. P.: Early Melt Season Variability of Fast Ice Degradation Due to Small Arctic Riverine Heat Fluxes, International Journal of Environmental and Ecological Engineering, 15, 9, 2021.

Schulson, E. M. and Hibler, W. D.: The fracture of ice on scales large and small: Arctic leads and wing cracks, Journal of Glaciology, 37, 319–322, https://doi.org/10.3189/S0022143000005748, 1991.

Segal, R. A., Scharien, R. K., Duerden, F., and Tam, C.-L.: The Best of Both Worlds: Connecting Remote Sensing and Arctic Communities for Safe Sea Ice Travel, Arctic, 73, 461–484, https://doi.org/10.14430/arctic71896, 2020.

Simonee, N., Alooloo, J., Carter, N. A., Ljubicic, G., and Dawson, J.: Sila Qanuippa? (How's the Weather?): Integrating Inuit Qaujimajatuqangit and Environmental Forecasting Products to Support Travel Safety around Pond Inlet, Nunavut, in a Changing Climate, Weather, Climate, and Society, 13, 933–962, https://doi.org/10.1175/WCAS-D-20-0174.1, 2021.

SmartICE: Tuvaliriji Meeting Minutes Sept. 26, 2022, ikpiarjuk, NU, Canada, 2022.

Statistics Canada: Provinces/Territories, Cartographic Boundary File - 2016 Census - Open Government Portal, https://open.canada.ca/data/en/dataset/a883eb14-0c0e-45c4-b8c4-b54c4a819edb, 2016.

Teigen, S. H., Høyland, K. V., and Moslet, P. O.: Thermal Stresses in First-Year Sea Ice, in: Proceedings of the 18th International Conference on Port and Ocean Engineering under Arctic Conditions, vol. 2, p. 14, 2005.

Timco, G. and Weeks, W.: A review of the engineering properties of sea ice, Cold Regions Science and Technology, 60, 107–129, https://doi.org/10.1016/j.coldregions.2009.10.003, 2010.

Timmermans, M.-L. and Marshall, J.: Understanding Arctic Ocean Circulation: A Review of Ocean Dynamics in a Changing Climate, Journal of Geophysical Research: Oceans, 125, e2018JC014 378, https://doi.org/10.1029/2018JC014378, 2020.

Tsamados, M., Feltham, D. L., Schroeder, D., Flocco, D., Farrell, S. L., Kurtz, N., Laxon, S. W., and Bacon, S.: Impact of Variable Atmospheric and Oceanic Form Drag on Simulations of Arctic Sea Ice, Journal of Physical Oceanography, 44, 1329–1353, https://doi.org/10.1175/JPO-D-13-0215.1, 2014.

Tucker, W. B. and Perovich, D. K.: Stress measurements in drifting pack ice, Cold Regions Science and Technology, 20, 119–139, https://doi.org/10.1016/0165-232X(92)90012-J, 1992.

Tuvaliriji Committee, Mike-Qaunaq, A., and Wilson, K.: Tuvaliriji Sea Ice Terminology, Tech. rep., SmartICE Sea Ice Monitoring and Information Services Inc., Ikpiarjuk, Canada, 2025.

Voermans, J. J., Liu, Q., Marchenko, A., Rabault, J., Filchuk, K., Ryzhov, I., Heil, P., Waseda, T., Nose, T., Kodaira, T., Li, J., and Babanin, A. V.: Wave dispersion and dissipation in landfast ice: comparison of observations against models, The Cryosphere, 15, 5557–5575, https://doi.org/10.5194/tc-15-5557-2021, 2021.

Weiss, J.: Sea Ice Fracturing, in: Drift, Deformation, and Fracture of Sea Ice: A Perspective Across Scales, edited by Weiss, J., SpringerBriefs in Earth Sciences, pp. 53–72, Springer Netherlands, Dordrecht, ISBN 978-94-007-6202-2, https://doi.org/10.1007/978-94-007-6202-2_4, 2013.

Weiss, J. and Dansereau, V.: Linking scales in sea ice mechanics, Philosophical transactions. Series A, Mathematical, physical, and engineering sciences, 375, 20150 352, https://doi.org/10.1098/rsta.2015.0352, 2017.

Weiss, J., Schulson, E. M., and Stern, H. L.: Sea ice rheology from in-situ, satellite and laboratory observations: Fracture and friction, Earth and Planetary Science Letters, 255, 1–8, https://doi.org/10.1016/j.epsl.2006.11.033, 2007.

https://doi.org/10.5194/egusphere-2026-3739
Preprint. Discussion started: 2 July 2026

Willmes, S. and Heinemann, G.: Sea-Ice Wintertime Lead Frequencies and Regional Characteristics in the Arctic, 2003–2015, Remote Sensing, 8, 4, https://doi.org/10.3390/rs8010004, number: 1 Publisher: Multidisciplinary Digital Publishing Institute, 2016.

Willmes, S., Heinemann, G., and Schnaase, F.: Patterns of wintertime Arctic sea-ice leads and their relation to winds and ocean currents, The Cryosphere, 17, 3291–3308, https://doi.org/10.5194/tc-17-3291-2023, publisher: Copernicus GmbH, 2023.

Wilson, K., Bell, T., Arreak, A., Koonoo, B., Angnatsiak, D., and Ljubicic, G.: Changing the role of non-Indigenous research partners in practice to support Inuit self-determination in research, Arctic Science, 6, 127–153, https://doi.org/10.1139/as-2019-0021, 2020.

Wilson, K. J., Arreak, A., Itulu, J., Ljubicic, G. J., and Bell, T.: "When We're on the Ice, All We Have is Our Inuit Qauji-majatuqangit": Mobilizing Inuit Knowledge as a Sea Ice Safety Adaptation Strategy in Mittimatalik, Nunavut, Arctic, 74, 25, https://doi.org/10.14430/arctic74212, 2021.

WMO: WMO Sea Ice Nomenclature, Tech. Rep. 259, WMO, https://library.wmo.int/doc_num.php?explnum_id=4651, 2014.